

1 **Origin and evolution of the Zinc Finger Antiviral Protein**

2

3

4 Daniel Gonçalves-Carneiro¹, Matthew A. Takata¹, Heley Ong¹, Amanda Shilton¹, Paul D.

5 Bieniasz^{1,2}

6

7 ¹Laboratory of Retrovirology, The Rockefeller University, New York, NY 10065

8 ²Howard Hughes Medical Institute, The Rockefeller University, New York, NY 10065

9

10 *corresponding author: pbieniasz@rockefeller.edu, 212-327-8848

11 **Abstract**

12 The human zinc finger antiviral protein (ZAP) recognizes RNA by binding to CpG
13 dinucleotides. Mammalian transcriptomes are CpG-poor, and ZAP may have evolved to
14 exploit this feature to specifically target non-self viral RNA. Phylogenetic analyses reveal that
15 ZAP and its paralogue *PARP12* share an ancestral gene that arose prior to extensive
16 eukaryote divergence, and the ZAP lineage diverged from the *PARP12* lineage in tetrapods.
17 Notably, The CpG content of modern eukaryote genomes varies widely, and ZAP-like genes
18 arose subsequent to the emergence of CpG-suppression in vertebrates. Human PARP12
19 exhibited no antiviral activity against wild type and CpG-enriched HIV-1, but ZAP proteins from
20 several tetrapods had antiviral activity when expressed human cells. In some cases, ZAP
21 antiviral activity required a TRIM25 protein from the same or a related species, suggesting
22 functional co-evolution of these genes. Indeed, a hypervariable sequence in the N-terminal
23 domain of ZAP contributed to species-specific TRIM25 dependence in antiviral activity assays.
24 Crosslinking immunoprecipitation coupled with RNA sequencing revealed that ZAP proteins
25 from human, mouse, bat and alligator exhibit a high degree of CpG-specificity, while some
26 avian ZAP proteins appear more promiscuous. Together, these data suggest that the CpG-
27 rich RNA directed antiviral activity of ZAP-related proteins arose in tetrapods, subsequent to
28 the onset of CpG suppression in certain eukaryote lineages, with subsequent species-specific
29 adaptation of cofactor requirements and RNA target specificity.

30

31 **Author Summary**

32 To control viral infections, cells have evolved a variety of mechanisms that detect, modify and
33 sometimes eliminate viral components. One of such mechanism is the Zinc Finger Antiviral
34 Protein (ZAP) which binds RNA sequences that are rich in elements composed of a cytosine
35 followed by a guanine. Selection of viral RNA can only be achieved because such elements
36 are sparse in RNAs encoded by human genes. Here, we traced the molecular evolution of
37 ZAP. We found that ZAP and a closely related gene, PARP12, originated from the same

38 ancestral gene that existed in a predecessor of vertebrates and invertebrates. We found that
39 ZAP proteins from mammals, birds and reptiles have antiviral activity but only in the presence
40 of a co-factor, TRIM25, from the same species. ZAP proteins from birds were particularly
41 interesting since they demonstrated a broader antiviral activity, primarily driven by relaxed
42 requirement for cytosine-guanine. Our findings suggest that viruses that infect birds – which
43 are important vectors for human diseases – are under differential selective pressures and this
44 property may influence the outcome of interspecies transmission.

45

46 **Introduction**

47 Organisms have evolved numerous mechanisms to detect and control viral infections. For
48 example, pattern recognition receptors (PRRs), including RIG-I-like receptors and Toll-like
49 receptors, can recognize RNA or DNA structures that are uniquely present or inappropriately
50 localized in virus-infected cells (1). Recognition by PRRs triggers a signalling cascade that
51 culminates in the increased transcription of many so-called interferon-stimulated genes
52 (ISGs), some of which encode effectors with direct antiviral properties (2). PRRs, signalling
53 molecules and direct antiviral effectors often exhibit species-dependent sequence and
54 functional divergence, as a natural consequence of extreme reciprocal selective pressures
55 placed on hosts and the viruses that colonize them.

56 The zinc finger antiviral protein (ZAP) is unusual in that it combines features of a
57 nucleic acid PRR and a direct antiviral effector. ZAP was initially found to inhibit the replication
58 of broad range of unrelated viruses, and to act by destabilizing viral RNA (3–5). Human ZAP
59 is composed of three structural domains: an N-terminal RNA-binding domain that has four
60 CCCH-type zinc fingers, a central domain that has an additional CCCH-type zinc finger plus
61 two WWE domains, and a C-terminal poly(ADP-ribose)-polymerase (PARP)-like domain. ZAP
62 requires certain cofactors for its antiviral activity, including TRIM25, a E3 ubiquitin ligase that
63 interacts with ZAP via its SPRY domain (6,7). However, the precise role of TRIM25 in ZAP
64 function is unknown. Several helicases and ribonucleases, including the putative
65 endonuclease KHNYN, have also been reported to be required for ZAP activity (8,9).

66 We recently showed that ZAP targets particular RNA elements based on their
67 dinucleotide composition (10). Specifically, ZAP binds directly to RNA elements that contain
68 CpG dinucleotides, and RNAs that contain CpG-rich sequences exhibit cytoplasmic depletion
69 in the presence of ZAP. X-ray crystal structures of the N-terminal RNA binding domain in a
70 complex with an RNA target have revealed that the specificity of ZAP for CpG dinucleotides
71 is conferred by a binding pocket positioned within a larger RNA binding domain (11,12). This
72 pocket can only accommodate CpG dinucleotides, and its integrity is required for specific

73 binding to CpG-rich RNA. Accordingly, the CpG content of viral genomes predicts their
74 sensitivity/resistance to ZAP (10).

75 Human ZAP has minimal effects on the host transcriptome, presumably because CpG
76 dinucleotides have been largely purged from the human genome, rendering human mRNAs
77 largely ZAP-resistant. The purging of CpG dinucleotides (or 'CpG-suppression') from host
78 genomes has occurred through DNA methylation followed by spontaneous deamination at
79 CpG dinucleotides over millions of years and to varying degrees in different lineages (13). A
80 commonly accepted theory that would enable this phenomenon argues that the emergence of
81 DNA methyltransferases – enzymes that catalyse the conversion of cytosines in a 5'-cytosine-
82 guanine-3' (CpG) context to 5-methyl-cytosine – led to increased levels of methylated CpG.
83 While spontaneous deamination of the methylated cytosine generates thymine, an authentic
84 DNA base, deamination of an unmethylated cytosine generates deoxyuridine, that would be
85 repaired. Thus, many DNA genomes have become purged of CpG dinucleotides and enriched
86 in TpG dinucleotides (14).

87 Remarkably, the genomes of many RNA viruses are CpG-poor, and to a large extent
88 CpG suppression in host is mirrored by CpG suppression in the viruses that colonize them.
89 This feature is true even for RNA viruses whose genome composition could not have been be
90 shaped by DNA methylation/deamination. The selective pressures that led to CpG
91 suppression in viral genomes remain unknown, but long-term adaptation to hosts in which a
92 selective pressure was imposed by ZAP is a likely possibility.

93 Here we investigated the origins of ZAP and its CpG-specific antiviral activity. A
94 paralogue of ZAP, *PARP12*, exists that also lacks poly(ADP-ribose) polymerase activity, but
95 catalyses the addition of mono(ADP-ribose) to proteins (15). Like ZAP, *PARP12* also contains
96 five CCCH-type zinc fingers, two WWE domains and has been reported to exhibit antiviral
97 activity against several RNA viruses including vesicular stomatitis virus (VSV), ECMV and
98 Dengue virus (16–18). Since *ZAP* and *PARP12* share domain and sequence homology, it is
99 likely that these antiviral genes have share the same ancestral gene. However, when this

100 gene duplication occurred and when specific CpG-binding affinity of ZAP-like proteins
101 emerged remains unknown. We examined the genomes of vertebrates and invertebrates for
102 gene products with sequence and domain homology to ZAP/PARP12. Phylogenetic analysis
103 of *ZAP/PARP12*-related sequences showed that these genes arose early in the divergence of
104 vertebrates and have their origin in an ancestral gene whose decedents are present in some
105 modern invertebrates, such as cnidarians, but absent in others, such as arthropods. Each of
106 the ZAP -related proteins from tetrapods that were examined showed antiviral activity against
107 CpG-enriched HIV-1 when overexpressed in human cells. Notably, in some cases co-
108 expression of a cognate TRIM25 protein in human cells was essential for the activity of ZAP
109 proteins from non-mammalian species (e.g., chicken and alligator) suggesting that these
110 proteins have co-evolved. Finally, we found that while CpG targeting specificity is common
111 among ZAP proteins of human, mouse, bats and alligator origin, ZAP proteins of avian origin
112 were less specific for CpG enriched targets and inhibited the replication of both wild type and
113 mutant HIV-1. These data suggest lineage-specific evolution of ZAP and its cofactors with
114 distinct non-self RNA targeting abilities that could influence the host range of viruses with
115 zoonotic potential.

116

117 **RESULTS**

118

119 **The dinucleotide composition of mRNAs and the origin of ZAP-like genes**

120 To understand the evolutionary origins of ZAP-mediated, CpG-rich RNA targeted, non-self
121 RNA recognition, we first mined vertebrate and invertebrate genomes for gene products with
122 sequence homology to human ZAP. In the human genome, a *ZAP* homolog, *PARP12*, that
123 shares several features with ZAP including five CCCH-type zinc fingers, two WWE domains
124 and a C-terminal PARP domain (**Fig 1A, S1 Fig A and B**), is found at a proximal location on
125 chromosome 7 (**Fig 1B**) , suggesting that *ZAP* and *PARP12* are paralogs that arose from a
126 common ancestor. A related gene termed 'ZAP-like' is present on human chromosome 7 but

127 contains sequences corresponding only to the ZAP N-terminal RNA binding domain (**Fig 1A**,
128 **S1 Fig A and B**). For searches of other genomes we considered sequences that contained
129 five CCCH-type zinc fingers and a WWE domain in a ZAP/PARP12-like configuration (**Fig**
130 **1A**). Most of the sequences revealed by blast searches also encoded PARP-like domains, in
131 common with ZAP and PARP12, but the PARP domain was lacking in ZAP/PARP12
132 sequences from a few species. The topology of a phylogenetic tree constructed using
133 ZAP/PARP12 protein sequences revealed two separate lineages in vertebrates and
134 invertebrates (**Fig 1C**) suggesting that a gene that is ancestral to modern *ZAP/PARP12*
135 originated prior to the divergence of cnidarians from other animals, approximately 650 million
136 years ago. While *ZAP/PARP12*-related sequences were found in several invertebrate
137 genomes, the *Arthropoda* phylum, which includes insects and nematodes, appeared to lack
138 *ZAP/PARP12* homologs, suggesting loss of *ZAP/PARP12* in this lineage.

139 Invertebrate genomes typically contained only one copy of a *ZAP/PARP12*-related
140 gene, while vertebrates had two (**Fig 1B, C**). One set of *ZAP/PARP12* related sequences were
141 more closely related to PARP12, and appeared to be represented once in tetrapod genomes
142 and twice in the genomes of several fish genomes (**Fig 1 B and C, S1 Fig C**), suggesting at
143 least one duplication event that was preserved in fish lineages. A clearly distinguishable set
144 of *ZAP/PARP12* genes emerged exclusively in tetrapods, and this lineage contained the human
145 *ZAP* gene that has been demonstrated to exhibit antiviral activity against CpG-rich viruses
146 (**Fig 1C**). Within tetrapods, the *ZAP*-related genes were more diverse in sequence than the
147 PARP12-related sequences (**Fig 1C, S1 Fig C**). Overall these data suggest that *ZAP*
148 originated in tetrapods from the duplication of an ancestral *PARP12* gene, and that *ZAP* may
149 have been under stronger diversifying selective pressure than *PARP12* (19).

150 Consistent with the aforementioned scenario, *ZAP* is located at about 900kb upstream
151 of *PARP12* in mammalian genomes, while *ZAP* and *PARP12* are further apart but on the same
152 chromosome in reptilian and avian genomes (**Fig 1B**). In the zebrafish genome, duplicated
153 *PARP12a* and *PARP12b* genes are located on two different chromosomes (18 and 4,

154 respectively, **Fig 1B**). The *PARP12a* locus resembles the *PARP12* locus in birds and reptile
155 while the *PARP12b* locus resembles that of *ZAP* in mammalian genomes (**Fig 1B**). Thus, even
156 though CpG-suppression is commonly observed among vertebrates, the genes most closely
157 related to human *ZAP* are found only in tetrapods (mammals, birds and reptiles).

158

159 **Human PARP12 does not recognize or inhibit expression from CpG-rich RNA**

160 Since *ZAP* and *PARP12* share an ancestral origin and are structurally related (**Fig 1**),
161 we inquired if *PARP12* also had antiviral activity against CpG-enriched HIV-1. To assess this,
162 we measured the infectious virus yield and viral protein expression in HEK293T *ZAP*^{-/-} cells
163 co-transfected with wild-type HIV-1 (*HIV-1*_{WT}) or CpG-enriched mutant (*HIV-1*_{CG}) proviral
164 plasmids and increasing amounts of plasmids expressing either human *ZAP*-L or human
165 *PARP12*. Increasing levels of *ZAP*-L reduced *HIV-1*_{CG} Env levels and the yield of infectious
166 *HIV-1*_{CG} but did not affect *HIV-1*_{WT}, as expected, but *PARP12* had no effect on the yield or
167 protein expression by either virus (**Fig 2A and B**). To test effects on other CpG-enriched or
168 CpG-suppressed virus derived sequences, we used a luciferase-based reporter system in
169 which *ZAP* or *PARP12* expression plasmids were cotransfected with a plasmid encoding the
170 firefly luciferase gene and a 3' UTR containing vesicular stomatitis virus (VSV) or influenza A
171 virus (IAV) derived sequences (**Fig 2C**). Plasmids that encoded CpG-enriched derivatives of
172 these sequences were included in the experiment (10). Overexpression of *ZAP* specifically
173 reduced the expression of the reporter gene with CpG-enriched 3'UTR sequences; however,
174 *PARP12* had no effect (**Fig 2C**). Thus, while they are structurally related, *PARP12* does not
175 share the same antiviral activity as *ZAP*. Differences in antiviral activity or specificity may be
176 attributable to variation in RNA-binding activity, as *ZAP*:RNA adducts were easily detected in
177 crosslinking immunoprecipitation assays, while *PARP12*:RNA adducts were undetectable
178 under the same experimental conditions (**Fig 2D**).

179

180 These data suggest the that CpG-specific antiviral activity emerged concurrently with or after
181 the emergence of the ZAP-like genes from a ZAP/PARP12 ancestral progenitor. To assess
182 whether the emergence of ZAP-like proteins was potentially enabled by the prior presence
183 CpG suppression in eukaryotic genomes, we generated an *in silico* library of open reading
184 frames (ORFs) and 3'UTRs from organisms across the tree of life, including: vertebrates,
185 nematodes, insects, molluscs and plants. We first calculated the frequency distribution
186 (observed/expected) for each of the 16 possible dinucleotides in ORFs (**Fig 3A**). Notably,
187 dinucleotide frequencies among distantly related species were similar, with the exception of
188 the dinucleotide CpG. Specifically, ORF sequences from arthropods and nematodes had CpG
189 frequencies close to that expected based on their mononucleotide compositions. Conversely,
190 CpG dinucleotides were suppressed in vertebrates (*Chordata*) and molluscs (*Mollusca*) (**Fig**
191 **3A and B**). CpG suppression was even more evident in vertebrate mRNA 3'UTRs (**Fig 3C**
192 **and S2 Fig A**), while the presence of CpGs in 5'UTRs was variable, more so than any other
193 dinucleotide, perhaps reflecting the comparatively short length of many 5'UTRs and a role for
194 RNA structure in translation regulation (**Fig 3C**). Overall, these data indicate that CpG-
195 suppression is observed primarily in vertebrates, is not specific to coding sequences, and was
196 likely present in animals prior to the emergence of genes closely related to the human ZAP
197 CpG-specific antiviral gene.

198

199 **ZAP proteins from tetrapods have antiviral activity, but some require a cognate**

200 **TRIM25**

201 We next assessed whether the ZAP-related genes from tetrapods that share the highest
202 homology with human ZAP exhibit CpG-targeted antiviral activity. During initial experiments,
203 we found that the full-length ZAP proteins from various species were expressed at inconsistent
204 levels in human cells. Therefore, in an attempt to circumvent this confounding variable, we
205 constructed plasmids expressing chimeric proteins in which the N-terminal zinc finger domains
206 of mouse, bat, chicken and alligator ZAPs were fused to the remaining portions (including the

207 WWE and PARP-like domains) of human ZAP (**Fig 4A**). Importantly, the isolated N-terminal
208 domain of ZAP has been reported to be sufficient for antiviral activity (3) and is responsible
209 for RNA recognition. By constructing these chimeras we aimed to maintain the RNA-binding
210 specificity of ZAP proteins while also maintaining the putative regulatory functions of the WWE
211 and PARP-like domains of human ZAP. To test the activity of these chimeric proteins, we first
212 transfected HEK293T ZAP^{-/-} cells with proviral plasmids and increasing amounts of plasmids
213 encoding the various ZAP chimeras. Chimeric ZAP proteins with N-terminal domains (NTDs)
214 from human (huZAP) and bat (baZAP) had antiviral activity against HIV-1_{CG}, while ZAP
215 chimeras with NTD's derived from alligator (alZAP) and mouse (moZAP) were less potent, the
216 ZAP chimera with an NTD from chicken (chZAP) had little or no antiviral activity (**Fig 4B and**
217 **C**).

218 The failure of the non-mammalian ZAP NTD chimeras to function in human cells could
219 have been due to an absence of RNA recognition activity, or incompatibility with a required
220 cofactor in human cells. One important co-factor for ZAP is TRIM25 (6,7). Even though
221 HEK293T ZAP^{-/-} cells express TRIM25, the nature of the TRIM25-ZAP interaction and
222 specifically, the ZAP domain with which TRIM25 functionally interacts is unknown.

223 Therefore, we explored whether the ZAP NTD interacts with TRIM25. Experiments in
224 which ZAP-L and TRIM25 were overexpressed in HEK293T ZAP^{-/-} TRIM25^{-/-} cells (**Fig 5A**)
225 revealed that ZAP and TRIM25, could be co-immunoprecipitated, as previously reported (6).
226 Removing the TRIM25 SPRY domain (one truncated form was composed of the N-terminal
227 371 amino acids and the other was composed of the N-terminal 410 amino acids) dramatically
228 reduced the HIV-1_{CG}-specific antiviral activity of ZAP (**Fig 5B**), as well as the ability of TRIM25
229 to co-immunoprecipitate with ZAP, again consistent with prior reports (**Fig 5A,B**) (6). Next we
230 conducted coimmunoprecipitation experiments in which the ability of full-length human ZAP-
231 L, a truncated form of ZAP lacking the NTD (Δ ZnF ZAP-L) or a truncated form comprised only
232 of the NTD (ZAP 254) to coimmunoprecipitate with TRIM25 was compared (**Fig 5C**). While
233 full length ZAP and ZAP 254 coimmunoprecipitated with TRIM25, the inactive (**Fig 5D**)

234 truncated ZAP, lacking the NTD, failed to coimmunoprecipitate with TRIM25 (**Fig 5C**). This
235 data suggests that ZAP and TRIM25 functionally interact via the N-terminal ZAP zinc finger
236 domain and the C-terminal SPRY domain of TRIM25.

237 Since both the ZAP NTD and TRIM25 proteins can bind RNA (11,20,21), it was
238 possible that RNA might have a bridging function and be responsible for the interaction
239 between the two proteins. To explore this hypothesis, we generated a ZAP mutant (R74A,
240 R75A, K76A, hereafter referred to as ZAP RNA^{null}). Notably ZAP RNA^{null} bound undetectable
241 levels of RNA in crosslinking immunoprecipitation assays (**Fig 5E**). We transfected HEK293T
242 ZAP^{-/-} cells with plasmids expressing wildtype ZAP-L or the ZAP RNA^{null} mutant, lysed the
243 cells and treated the cell lysates with RNase A or a mixture of RNase A and T1 prior
244 immunoprecipitation (**Fig 5F**). RNase A or A/T1 treatment only slightly affected
245 coimmunoprecipitation of ZAP with endogenous TRIM25. Furthermore, the ZAP RNA^{null}
246 mutation increased, rather than decreased, the amounts of coprecipitated endogenous
247 TRIM25. Similarly, in experiments where HEK293T ZAP^{-/-} TRIM25^{-/-} cells were cotransfected
248 with plasmids expressing wildtype or RNA-binding-defective mutants of ZAP (ZAP WT and
249 ZAP RNA^{null}) and TRIM25 (TRIM25 WT and TRIM25 7KA (20)), the amount of coprecipitated
250 TRIM25 did not suggest a role for RNA in mediating ZAP-TRIM25 interactions (**Fig 5G**).
251 Specifically, the amount of TRIM25 coprecipitated with ZAP was the same or increased when
252 either ZAP RNA^{null} or TRIM25 7KA mutants were expressed in place of the wild-type proteins.
253 Overall, these results suggest that ZAP NTD and TRIM25 interact in a manner that is
254 dependent on protein-protein rather than protein-RNA interactions.

255 Since human TRIM25 interacted with human ZAP in an NTD dependent manner, but
256 the ZAP chimeras encoded an NTD from a different species, it was possible that an inability
257 to functionally interact with endogenous human TRIM25 was responsible for their absent or
258 poor activity in of some ZAP chimeras in human cells. To explore this hypothesis, we tested
259 whether the expression of TRIM25 from various species could support the activity of ZAP
260 chimeras encoding a ZAP NTD from that species. TRIM25-related genes are present in

261 mammals, birds and reptiles and some species of fish (**Fig 6A**). To assess whether the
262 expression of cognate TRIM25 could augment the antiviral activity of each ZAP chimera, we
263 measured infectious HIV-1_{CG} yield from HEK293T ZAP^{-/-} TRIM25^{-/-} cells cotransfected with
264 plasmids expressing TRIM25 and chimeric ZAP proteins from various species (**Fig 6B**). While
265 there was some variation in potency, ZAP chimeras from mammalian species generally
266 exhibited antiviral activity in the presence of TRIM25, regardless of the species of origin.
267 Conversely ZAP proteins from more distantly related species (chicken and alligator) were
268 poorly active when coexpressed with mammalian TRIM25 proteins, but exhibited greater
269 antiviral activity when coexpressed with a TRIM25 protein from the same species (**Fig 6B**).

270 To test whether the ZAP NTD from the various species had the same or different target
271 RNA specificities, HEK293T ZAP^{-/-} and TRIM25^{-/-} were co-transfected with plasmids
272 expressing a ZAP chimera and a cognate TRIM25 protein, together with a HIV-1_{WT} or HIV-1_{CG}
273 proviral plasmid (**Fig 7A and B**). Interestingly, while all the ZAP/TRIM25 proteins reduced the
274 yield of HIV-1_{CG}, some of the TRIM25 and ZAP chimera combinations also reduced the yield
275 of HIV-1_{WT} to some extent. This was particularly the case for the chicken TRIM25 and ZAP
276 chimera combination which reduced the yield of infectious HIV-1_{WT} by >10 fold at the highest
277 dose tested, suggesting that ZAP from chicken might have a different or expanded RNA
278 binding specificity.

279 Birds comprise one of the most diverse phyla in vertebrates, with about 10,000
280 species, adapted to a wide range of habitats (22). Since chicken ZAP was phenotypically
281 distinct from other vertebrate ZAPs, we investigated whether ZAP from other species of birds
282 share a similar phenotype with chicken ZAP. We constructed chimeric ZAP proteins in which
283 the RNA binding domain was from one of several additional bird species: three from the order
284 *Galliformes* – chicken (*Gallus gallus*), turkey (*Meleagris gallopavo*) and duck (*Anas*
285 *platyrhynchos*) – and two from the suborder *Neoaves* – eagle (*Aquila chrysaetos canadensis*)
286 and zebra finch (*Taeniopygia guttata*) (**Fig 7C and D**). The avian ZAP chimeric proteins
287 exhibited different levels antiviral activity, but some, particularly the chicken and zebra finch

288 ZAP chimeras reduced HIV-1_{WT} yield (**Fig 7B and D**). Indeed, the zebra finch ZAP chimera
289 was nearly as potent against HIV-1_{WT} as it was against HIV-1_{CG}. These findings suggest that
290 a loss of selectivity for CG-rich RNA, or expansion of RNA target specificity has occurred on
291 more than one occasion in avian ZAP proteins.

292

293 **RNA-binding specificity of chicken and human ZAP proteins differs**

294 Since human ZAP binds to CG-rich RNA with high selectivity (10,11), differences in RNA
295 binding affinity and specificity might explain the altered antiviral specificity of some avian ZAP
296 proteins. We focused on chicken ZAP, and used crosslinking immunoprecipitation coupled
297 with RNA sequencing (CLIP-Seq) to determine its RNA-binding preference in HEK293T ZAP⁻
298 ⁻ TRIM25⁻ cells cotransfected with an HIV-1_{CG} proviral plasmid along with plasmids encoding
299 human or chicken ZAP. This analysis revealed that, as expected and previously reported (10),
300 human ZAP bound primarily to regions of the genome that contained a high number of CG
301 dinucleotides (**Fig 8A**). Notably, the chicken chimeric ZAP preferentially bound to the CG-rich
302 portion of the viral genome, but also exhibited a comparatively higher level of binding to the
303 CpG-poor portions of the viral genome. We quantified the representation of each of the 16
304 dinucleotides in ZAP-crosslinked total reads from the viral genome for both human and
305 chicken ZAP (**Fig 8B**). While CpG dinucleotides were enriched in RNAs crosslinked to both
306 chicken and human ZAP chimeras, CpG enrichment was clearly less pronounced in chicken
307 ZAP. Together these data suggest that chicken ZAP is less selective toward CG-rich RNA and
308 this property correlates with the broader antiviral activity of chicken ZAP.

309

310 **A determinant in the ZAP NTD that governs species-specific TRIM25 dependence**

311 The maximal antiviral activity of the chicken ZAP NTD chimera requires chicken TRIM25. In
312 an attempt to determine what region in the ZAP NTD is responsible for this species-specific
313 dependence, we inspected aligned protein sequences from human and chicken ZAP NTDs.
314 We noticed that a divergent protein sequence, composed of two predicted α -helices is present

315 in the C-terminal portion of the NTD (**Fig 9A, B**). Based on the crystal structure of human ZAP
316 (11), these α -helices are located proximal to the third and fourth zinc fingers, facing away from
317 the RNA-binding pocket (**Fig 9A**). To test whether this element is important for species-
318 specific TRIM25 dependence, we generated a chimera that contained the four N-terminal zinc
319 fingers from chicken ZAP, and the divergent NTD α -helices from the human ZAP (chZAP-X,
320 **Fig 9B**). We compared the activity of chZAP-X with that of the human ZAP, and the previously
321 constructed chZAP chimera in the presence of human or chicken TRIM25 (**Fig 9C**). As
322 previously observed, human ZAP was active against HIV-1_{CG} in the presence of either human
323 or chicken TRIM25. Conversely, the original chZAP chimera was more potent in the presence
324 of chicken TRIM25 than human TRIM25, and also exhibited activity against HIV-1_{WT} in the
325 presence of chicken TRIM25 (**Fig 9C**). Notably, the chZAP-X chimera, was more active
326 against HIV-1_{CG} than chZAP in the presence of human TRIM25. Moreover, chZAP-X was also
327 active against HIV-1_{WT} in the presence of either human or chicken TRIM25. Overall these data
328 indicated that the four NTD zinc fingers of chicken ZAP are responsible for the its expanded
329 antiviral activity against HIV-1_{WT}, while the two divergent NTD α -helices are at least partly
330 responsible for the species-specific dependence of chicken ZAP protein on chicken TRIM25.

331

332

333 **DISCUSSION**

334 The emergence of genes with new functions is central to the adaptability of organisms
335 to new challenges. Viral infections impose a strong selective pressure on their hosts, thus
336 gene products with antiviral functions constitute prominent examples of genetic innovation and
337 are among the fastest evolving genes (23). While our analysis suggests that *ZAP* originated
338 from a duplication of the *PARP12* gene, and both human *PARP12* and *ZAP* have been
339 reported to exert antiviral activity against a broad range of viruses, the mechanisms by which
340 they exert their function are different. Specifically, *ZAP* antiviral function is primarily
341 related to their RNA recognition (3,4,10), while *PARP12* showed no detectable RNA-binding

342 activity. Indeed previous work has indicated that PARP12 antiviral activity is linked to PARP
343 domain-dependent ADP-ribosylation of viral proteins (16,24). The PARP-like domain of
344 mammalian ZAP proteins is catalytically inactive, and therefore, cannot catalyze ADP-
345 ribosylation of viral or endogenous proteins (25,26). Interestingly, however, sequence
346 alignments of PARP domains of chicken and alligator ZAP, revealed that these ZAP proteins
347 likely contain catalytically active PARPs, raising the possibility that these are bifunctional
348 antiviral proteins. A more recent gene duplication has apparently occurred in mammals, as
349 revealed by the existence of another paralogue of ZAP, termed ZAP-like or *ZC3HAV1L*. This
350 gene encodes a shorter protein, that contains four CCCH-type zinc fingers and appears
351 paralogous to the ZAP RNA-binding domain (**S1 Fig**). Since the ZAP RNA-binding domain is
352 sufficient to inhibit virus replication (3), it is plausible that *ZC3HAV1L* has antiviral activity.
353 However, this awaits definitive experimentation.

354 Our prior work suggests that ZAP exploits the CpG suppressed state of human
355 genomes to discriminate between self and non-self RNA (10). CpG suppression in animal
356 genomes is thought to be the by-product of DNA methylation and subsequent deamination of
357 5-methyl-cytosine into thymidine, followed by the repair of the mispaired G on the opposing
358 strand (13). Thus, the extent to which CpG dinucleotides in a given genome is methylated is
359 linked to the degree of CpG suppression therein. Indeed, while the dinucleotide frequency
360 distributions are similar for most dinucleotides in most organisms, CpG dinucleotide frequency
361 in animal genomes can vary widely (**Fig 3A**). In particular, the coding sequences of several
362 vertebrates (mammals, birds, reptiles, fish) and some non-arthropod invertebrates (molluscs)
363 show substantial levels of CpG suppression, while in arthropods, nematodes and some
364 species of plants the frequency of CpG dinucleotides is higher. This property correlates with
365 the extent of DNA methylation observed in these organisms (27). Thus, the CpG suppressed
366 state of animal genomes creates the opportunity for self-nonsel self discrimination by ZAP-related
367 proteins that has apparently been exploited in tetrapods. Nevertheless, one study showed the
368 rate of CpG DNA methylation in genomes may be insufficient to explain the extent to which

369 vertebrate mRNA is CpG-suppressed (28). Indeed, RNA transcripts in some organisms seem
370 to be under additional selective pressures to purge CpG dinucleotides, as suggested by the
371 observed frequency of C-to-A mutations in a CpG context. Thus, it is possible that the
372 emergence of ZAP/PARP12 related genes may have further shaped the dinucleotide
373 composition of coding sequences in modern genomes.

374 We found that the activity of ZAP proteins from different organisms was inherently
375 dependent on the cellular context. Indeed, in line with previous reports (6,7) we found that the
376 expression of a ZAP cofactor, TRIM25, was important for its antiviral activity against CpG-
377 enriched HIV-1. In fact, the activity of ZAP proteins from certain species (chicken and alligator)
378 was dependent on the coexpression of a cognate TRIM25 protein. This species-specific
379 dependency suggests that ZAP and TRIM25 interact in a way that is maintained across
380 different species. Concordantly, replacing two poorly conserved, α -helices immediately C-
381 terminal to the RNA binding domain in chicken ZAP with the equivalent element from human
382 ZAP enabled the chimeric protein to function better in the presence of human TRIM25. This
383 result strongly suggests a species-specific component of the interaction between ZAP and
384 TRIM25. Consistent with this finding, prior work, confirmed herein, has suggested a physical
385 interaction between ZAP and TRIM25 in a manner that was dependent on the TRIM25 SPRY
386 domain (6). Additionally, we showed that the ZAP NTD, that includes the RNA binding domain,
387 is necessary and sufficient to co-immunoprecipitate TRIM25. Notably, two domains in TRIM25
388 have been reported to bind RNA: (1) a short section of positively-charged amino acids located
389 between the coiled-coil domain and the PRY/SPRY domain (N- KKVSKEEKSKK-C, amino
390 acids 381-391 (20)), and (2) a small region (470-508) within the PRY/SPRY domain (21)).
391 Additionally, two reports suggested that RNA enhances the E3-ubiquitin ligase activity of
392 TRIM25 *in vitro* (20,21). However, we found that a TRIM25 mutant in which the lysine cluster
393 at 381-391 was replaced by alanines (TRIM25 7KA) supported antiviral activity. Moreover,
394 TRIM25 7KA, ZAP-RNA^{Null} and RNaseA/T1 treatment were all compatible with ZAP-TRIM25
395 coprecipitation. Together, these results suggest that ZAP-TRIM25 interaction is not RNA-

396 dependent and is likely mediated by protein-protein contacts. That there exists a species-
397 specific restriction in ZAP-TRIM25 functional compatibility, that can be mapped to a specific
398 protein element, is consistent with this notion.

399

400 Finally, we found that avian ZAP proteins, unlike human ZAP, exhibit varying degrees of
401 antiviral activity against HIV-1_{WT} as well as HIV-1_{CG}. Consistent with this finding, CLIP-Seq
402 analysis using chicken ZAP revealed that it binds more promiscuously throughout the viral
403 genome than does human ZAP. Recently, two structures of ZAP (from human and mouse)
404 bound to a target RNA elucidated the nature of the interaction between ZAP and CG
405 dinucleotides (11,12). Key contacts are established by ZAP residues K89, Y98, K107 and
406 Y108 (11). Of these, K89, K107 and Y108 are conserved between human and chicken ZAP.
407 Notably, the second zinc finger of chicken ZAP is three-amino acids shorter than the human
408 counterpart; how the structural divergence between these human and avian ZAP influences
409 RNA binding specificity required further investigation, but mutations at various positions
410 surrounding the CpG binding pocket in human ZAP can cause relaxation in strict CpG
411 specificity (11). Interestingly, birds are important vectors for certain human viral infections,
412 such as influenza and West Nile virus. The CpG dinucleotide content of influenza A viruses
413 has progressively decreased in human populations following zoonotic transmission from birds
414 (29). Moreover, the frequency of CG dinucleotides in viral genomes can be used to predict
415 animal reservoirs (30). In the case of birds, viruses that infect *Neoaves* – and to some extent
416 viruses that infect *Galliformes* – have higher CpG dinucleotide frequencies than viruses that
417 infect primates or rodents. Together, our results provide a potential molecular explanation for
418 the observed fluctuations in CpG-content of viruses that have adapted to different hosts, and
419 suggest that ZAP's antiviral activity represents a selective pressure that influences the
420 dinucleotide composition of viral genomes.

421 Overall, these findings highlight the potential for innovation of gene function driven by
422 viral infection. Understanding how different organisms have evolved to control infections will

423 illuminate the mechanisms of host range restriction and enable novel interventions in viral
424 diseases.

425

426 **Materials and Methods**

427

428 **Cells**

429 Human embryonic kidney (HEK) 293T, HEK293T ZAP^{-/-} (10) , HEK293T ZAP^{-/-} TRIM25^{-/-} (6)
430 and chicken fibroblasts DF1 (ATCC, CRL-12203) were cultured in Dulbecco's Modified
431 Eagle's Medium (DMEM) supplemented with foetal bovine serum (FBS). *Eptesicus fuscus*
432 kidney (EFK) cells were purchased from Kerafast, Inc (ESA001) and cultured in DMEM
433 supplemented with FBS. Mouse embryonic fibroblasts (MEFs, (31)) were cultured in DMEM
434 supplemented with bovine calf serum (BCS). MT4-R5-GFP cells (32) were grown in RPMI
435 medium supplemented with FBS. All cells were maintained at 37°C in 5% CO₂.

436

437 **Plasmids**

438 Sequences encoding the RNA-binding domains of alligator, turkey, duck, zebra finch and
439 eagle ZAP were retrieved from the NCBI nucleotide database and DNA was synthesised by
440 Twist Biosciences. Total RNA from EFK cells was extracted using the NucleoSpin RNA
441 purification kit (Macherey-Nagel) according to manufacturer's guidelines, reverse transcribed
442 into cDNA using the SuperScript III First-Strand Synthesis System (Invitrogen), and bat ZAP
443 was amplified using specific primers. TRIM25 mRNA was isolated from MEF, EFK, DF1 cell
444 lines, as above, and reverse transcribed to generate cDNA. Alligator, turkey, duck, zebra finch
445 and eagle TRIM25 cDNA was synthesised by Twist Biosciences. Total RNA from the intestine
446 of a zebrafish specimen (kindly provided by Professor A. James Hudspeth, The Rockefeller
447 University) was extracted and TRIM25 cDNA was generated as before. ZAP chimeras were
448 generated by fusing the RNA-binding domain of ZAP isolated from indicated species to the
449 residues 255-902 of the long isoform of human ZAP-L, that was C-terminally tagged with three

450 HA epitopes or one FLAG epitope, as indicated, and inserted into the expression plasmid
451 pCR3.1. TRIM25 sequences were fused to a C-terminal HA epitope and inserted into pCR3.1.
452 The two truncated versions of TRIM25 (1-371 and 1-410) and the TRIM25 7KA mutants were
453 a kind gift from Owen Pornillos, University of Virginia (20). The ZAP RNA^{null} mutant was
454 generated by introducing three point-mutations R74A, R75A and K76A. by overlap extension
455 PCR

456

457 **Bioinformatics**

458 The protein sequences of human ZAP and PARP12 were retrieved from GeneBank.
459 These sequences were subsequently used to identify orthologues in other species using the
460 Blastp suite of NCBI. Sequences with significant E-values were used for subsequent
461 sequence alignments and phylogenetic analysis. We considered the identified protein
462 sequences to be products of orthologues of *ZC3HAV1/PARP12* if (1) significant sequence
463 homology was observed, (2) if sequences contained 5 CCCH-type zinc fingers and (3) if WWE
464 and PARP-like domains were present. MUSCLE was used to perform multiple sequence
465 analysis. Phylogenetic trees were derived using BEAST (33) and plotted using FigTree.
466 Speciation dates were based on (34). A similar approach was taken to identify and analyse
467 *TRIM25* orthologues. For synteny studies, *ZC3HAV1/PARP12* loci from different vertebrate
468 species were analysed using Ensembl and Genomicus Browsers.

469 For nucleotide composition studies, RNA transcript sequences from human (*Homo*
470 *sapiens*), house mouse (*Mus musculus*), little brown bat (*Myotis lucifugus*), chicken (*Gallus*
471 *gallus*), alligator (*Alligator mississippiensis*), dog (*Canis familiaris*), zebrafish (*Danio rerio*),
472 California two-spot octopus (*Octopus bimaculoides*), oyster (*Crassostrea gigas*), mosquito
473 (*Aedes aegypti*), sandfly (*Lutzomyia longipalpis*), tick (*Ixodes scapularis*), pacific white shrimp
474 (*Litopenaeus vannamei*), *Caenorhabditis elegans*, coral (*Acropora digitifera*) and *Arabidopsis*
475 *thaliana* were retrieved from the NCBI nucleotide sequence database. Subsequently,
476 sequences were fragmented into 5' UTRs, ORFs and 3'UTRs. Mononucleotide and

477 dinucleotide frequencies were calculated using the SSE suite (35) and analysed using in-
478 house R scripts.

479

480 **Virus Yield Assays**

481 To assess the activity of different zinc finger proteins, virus yield was measured as described
482 previously(11). In brief, HEK293T ZAP^{-/-} TRIM25^{-/-} were seeded onto a 24-well plate and
483 transfected with 375ng of HIV-1_{WT} or HIV-1_{CG} proviral plasmids, along with 87ng of a plasmid
484 encoding TRIM25 and varying amount of ZAP expression constructs, unless otherwise
485 indicated. After 24h, media were replaced and at 48h post-transfection supernatants were
486 collected, filtered through a 0.22µm filter and titres determined using MT4-R5-GFP target
487 cells. Transfected cells were lysed in NuPAGE buffer and protein samples were analysed by
488 western blotting.

489

490 **Luciferase Assays**

491 Expression constructs encoding a recoded, low-CpG firefly luciferase and containing wildtype
492 or CG-enriched VSV-G or IAV-NP sequences as 3' UTRs were used to assess the activity of
493 ZAP and PARP12, as described before (10). Cells were co-transfected with 50ng of luciferase-
494 encoding plasmids, 250ng of plasmids encoding human ZAP-L or PARP12 and human
495 TRIM25. After 56h, cells were lysed in cell lysis buffer and luciferase activity was measured
496 using the Luciferase Assay System (Promega).

497

498 **Western Blotting**

499 Cell lysates were incubated at 72°C for 20min and sonicated for 20s. Protein samples were
500 resolved in a 4-12% PAGE gel (Novex) using MOPS running buffer. Protein was transferred
501 to a nitrocellulose membrane, blocked at room temperature and incubated with the following
502 antibodies: anti-ZC3HAV1 (rabbit, 1:10,000, clone 16820-1-AP, Proteintech Group), anti-
503 TRIM25, anti-HA (rabbit, 1:5000, clone 600-401-384, Rockland), anti-Tubulin (mouse,

504 1:10,000, clone DM1A T9026, Millipore-Sigma), anti-HIV-1 Env (goat, 1:1000, 12-6205-1,
505 American Research Products). Blots were washed and incubated with secondary antibodies:
506 anti-Mouse IgG IR700 Dye Conjugated (Licor), Anti-Rabbit IgG IR800 Dye conjugated (Licor),
507 Anti-Goat IgG IR800 Dye Conjugated (Licor) and Anti-Rabbit IgG horseradish peroxidase
508 conjugated (Jackson). Blots were imaged immediately in a Licor Odyssey scanner or
509 incubated with ECL substrate and imaged on a CDigit blot scanner.

510

511 **RNA-Protein Immunoprecipitation**

512 Cells were seeded onto a 15cm dish and transfected, 24h later, with 8 μ g of plasmids encoding
513 ZAP-L-3xHA, PARP12-3xHA or ZAP RNA^{Null} (R74A,R75A, K76A)-3xHA. The following day,
514 media were replaced by culture media containing 4-thiouridine. Two days after transfection,
515 cells were exposed to UVB light (0.15 J cm⁻², λ = 365 nm, Stratalinker 2400 UV), washed in
516 PBS and lysed in Lysis Buffer (10mM HEPES pH7.5, 30mM KCl, 40 μ M EDTA, 0.1% Igepal
517 CA-630 supplemented with protease inhibitor cocktails). Lysates were clarified by
518 centrifugation and incubated with RNase A for 5min at 37°C. Anti-HA mouse antibody
519 (BioLegend) was adsorbed to protein G agarose beads and incubated with the cell lysates for
520 2h at 4°C. Beads were washed twice in NP40 Lysis Buffer, twice IP wash buffer (50mM
521 HEPES pH 7.5, 300mM KCl, 2mM EDTA, 0.5% Igepal CA-630), twice in LiCl buffer (250mM
522 LiCl, 10mM Tris pH 8.0, 1mM EDTA, 0.5% Igepal CA-630, 0.5% sodium deoxycolate), twice
523 in NaCl Buffer (50mM Tris pH 7.5, 1M NaCl, 1mM EDTA, 0.1 SDS, 0.5% sodium
524 deoxycolate) and twice in KCl buffer (50mM HEPES pH 7.5, 500 mM KCl, 0.05% Igepal CA-
525 630). RNA:Protein complexes were incubated with calf intestinal phosphatase (NEB) for
526 13min at 37°C and washed in phosphatase wash buffer (50mM Tris HCl pH 7.5, 20mM EGTA,
527 0.5% NP40). Beads were resuspended in PNK buffer (50 mM Tris HCl pH 7.5, 50mM NaCl,
528 10mM MgCl₂) and incubated with 5 U of PNK in the presence of 0.5 μ Ci/ μ L γ -³²P ATP. Beads
529 were washed, lysed in NuPAGE Lysis buffer and RNA:Protein complexes were resolved in a

530 4-12% NuPAGE gel. Complexes were transferred to nitrocellulose membrane and exposed to
531 autoradiographic film.

532

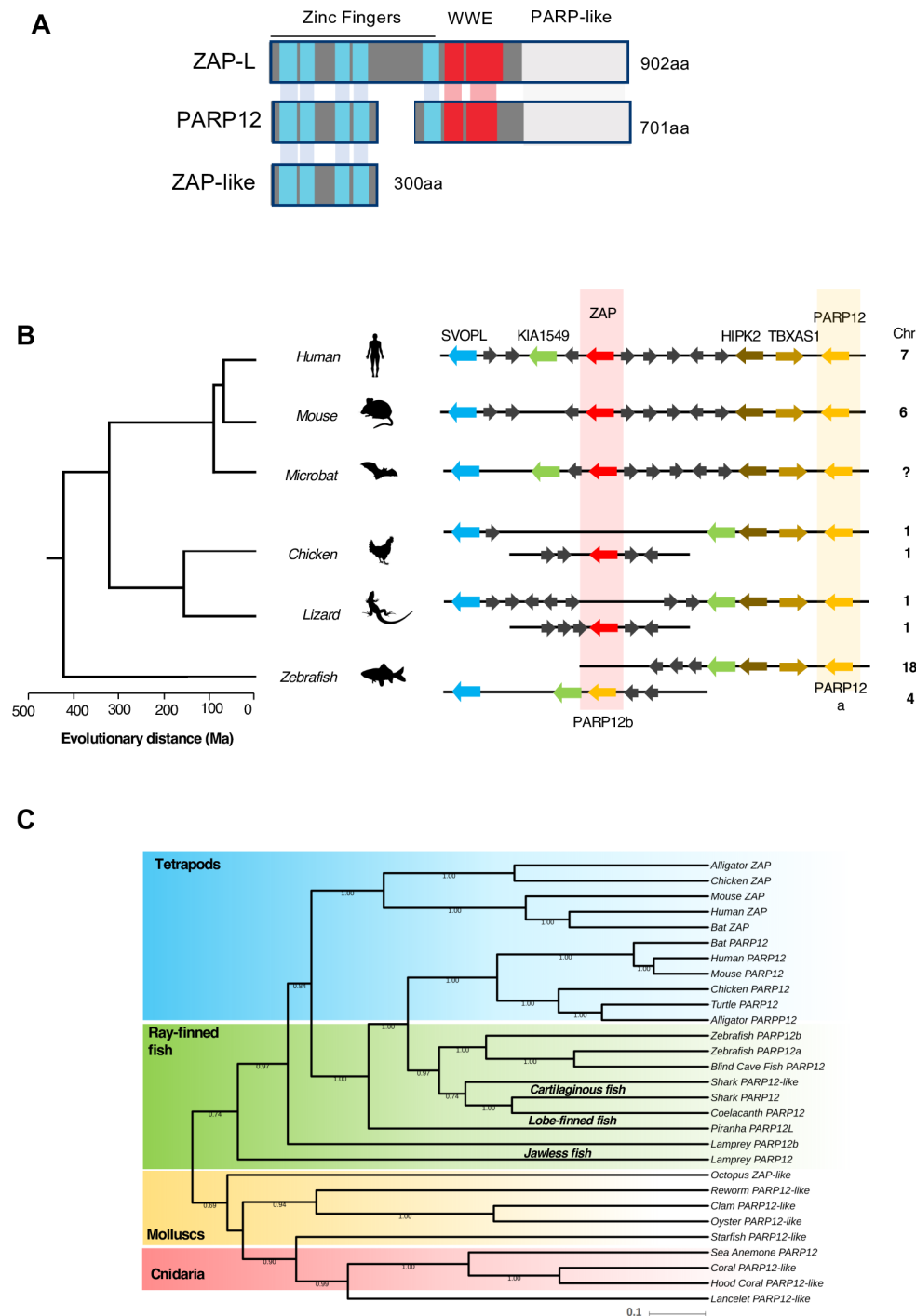
533 **Co-immunoprecipitation**

534 To evaluate ZAP and TRIM25 interactions, cells (HEK293T ZAP^{-/-} or HEK293T ZAP^{-/-} TRIM25^{-/-})
535 were seeded onto a 10cm dish and co-transfected, 24h later, with 3µg of a plasmid encoding
536 ZAP-FLAG and 3µg of a plasmid encoding TRIM25-3xHA. In experiments in which
537 endogenous TRIM25-positive cells were transfected, only ZAP-encoding plasmids were used.
538 Cells were lysed 48h after transfection in 1.5mL of Lysis Buffer (10mM HEPES pH7.5, 30mM
539 KCl, 40µM EDTA, 0.1% Igepal CA-630 supplemented with protease inhibitor cocktails).
540 Lysates were clarified by centrifugation and treated with RNase A (Roche, 100 Units) or
541 RNase A/T1 (NEB, 100 Units) for 5min at 37°C. Protein G agarose beads that were pre-
542 adsorbed to either anti-HA (BioLegend) or anti-FLAG (Millipore) antibodies were added to the
543 lysates and incubated at 4°C for 2h. Magnetic beads were captured and washed twice in lysis
544 buffer and three times in IP wash buffer (50mM HEPES pH 7.5, 300mM KCl, 2mM EDTA,
545 0.5% Igepal CA-630). Protein complexes were resuspended in NuPAGE buffer and resolved
546 on a 4-12% PAGE gel, transferred to nitrocellulose membranes and analysed by western
547 blotting.

548

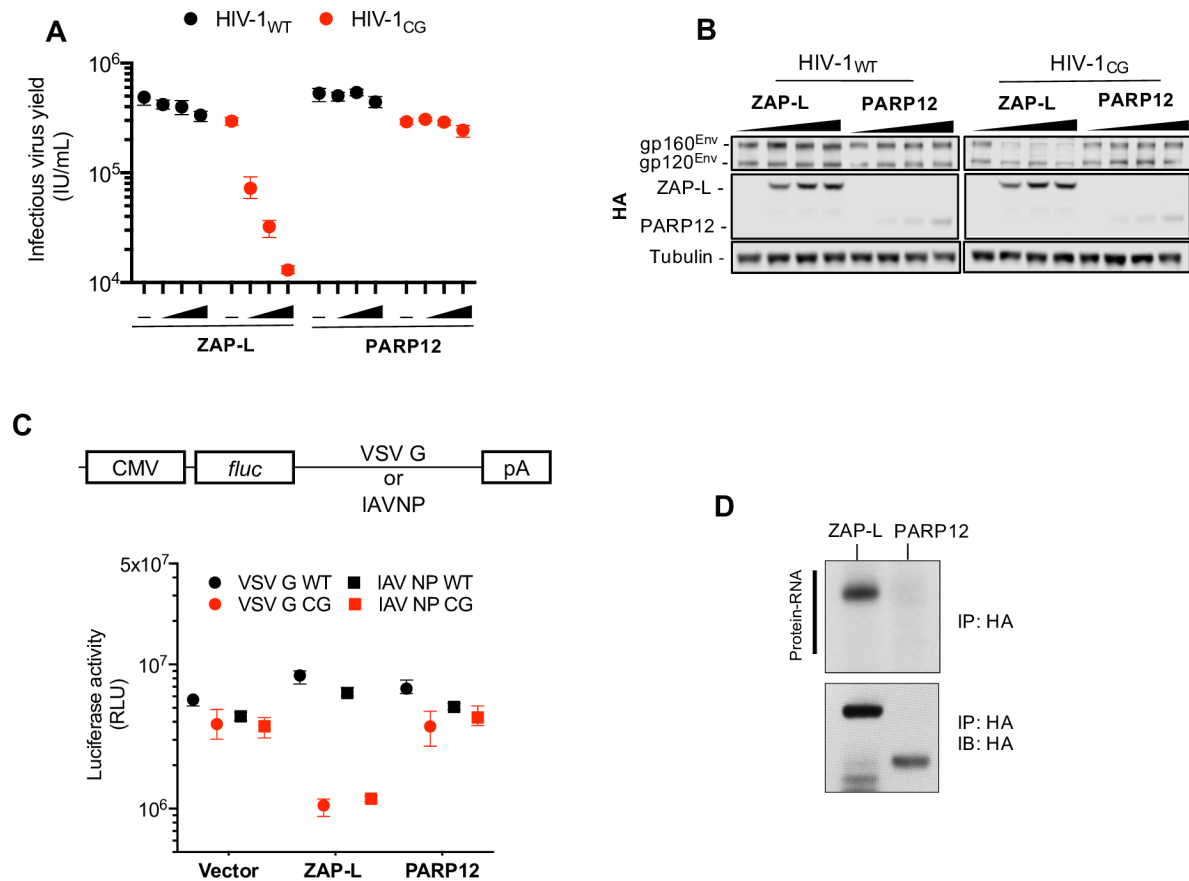
549 **CLIP-Seq**

550 RNA:protein complexes were isolated as described above. RNA was isolated and prepared
551 for sequencing as before (36). In brief, after isolation of RNA:protein complexes, RNA was
552 released using Proteinase K (Roche). Purified RNA fragments were ligated to 3' and 5'
553 adaptors, reverse transcribed (SuperScript First-Strand cDNA Synthesis System, Invitrogen)
554 and amplified by PCR. The resulting cDNA library was sequenced using the Illumina HiSeq
555 2000 platform. Sequencing reads were processed and analysed as described previously (10).
556



557

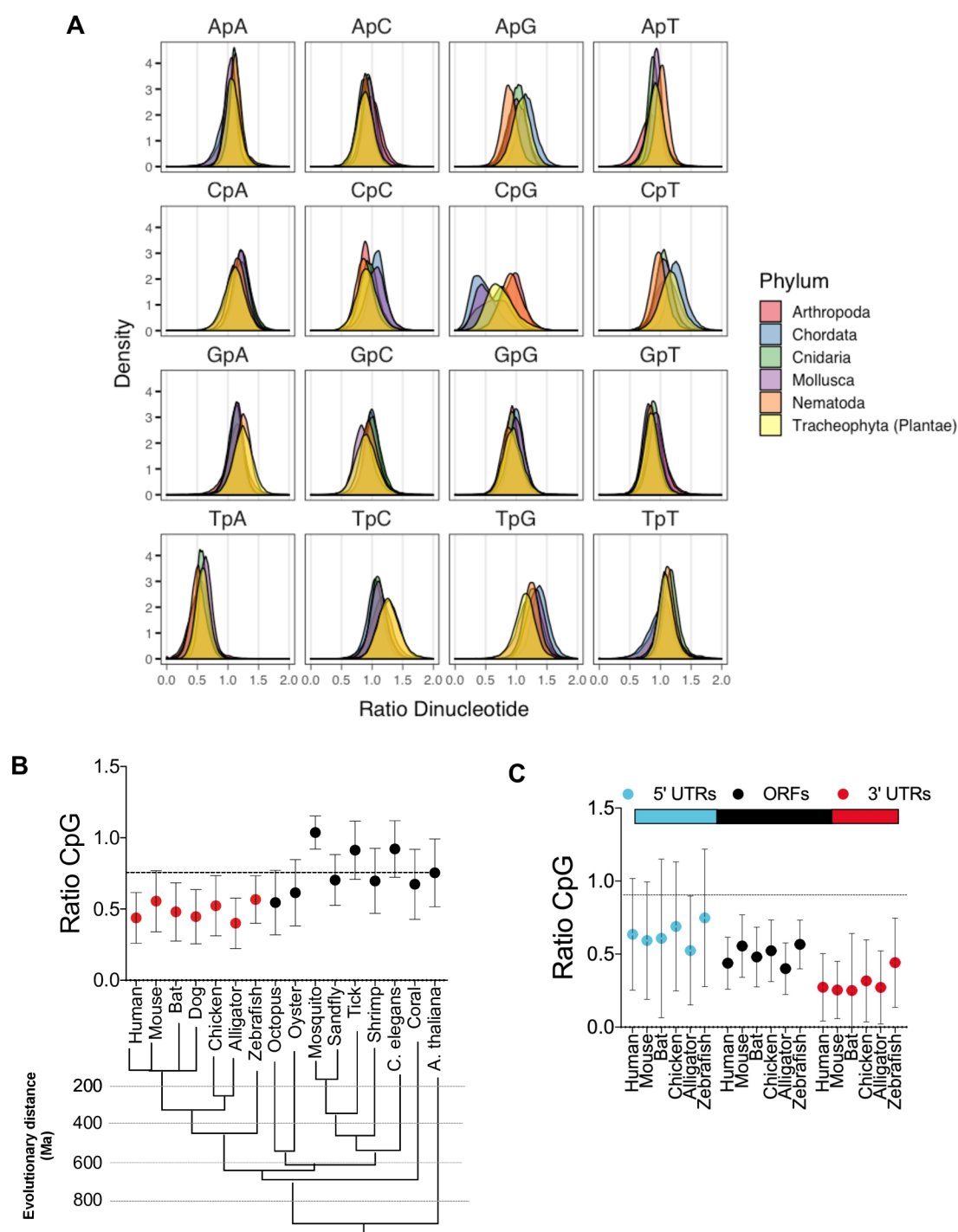
558 **Fig 1. ZAP and PARP12 share a common ancestor.** (A) Schematic representation of the
 559 domain organization of human ZAP and its paralogues PARP12 and ZAP-like. (B) Diagrams
 560 of the organization of PARP12 (in yellow) and ZAP (in red) loci in vertebrate genomes
 561 generated using multiple genome browsers (NCBI, Ensembl, Genomicus). Evolutionary
 562 distance of the indicated species (presented in million years, Ma) is based on (34). Chr,
 563 chromosome number. (C) Maximum likelihood tree (midpoint rooted) depicting phylogenetic
 564 relationships among *PARP12*- and *ZAP*-related genes in vertebrate and invertebrate species,
 565 generated with BEAST and 1000 bootstrap replicates. Shaded areas loosely cluster
 566 sequences from related species in the superclass Tetrapoda (in blue), clade Actinopterygii
 567 (Ray-finned fish, in green), the phylum Mollusca (molluscs, in yellow) and the phylum Cnidaria
 568 (in red).



569
570

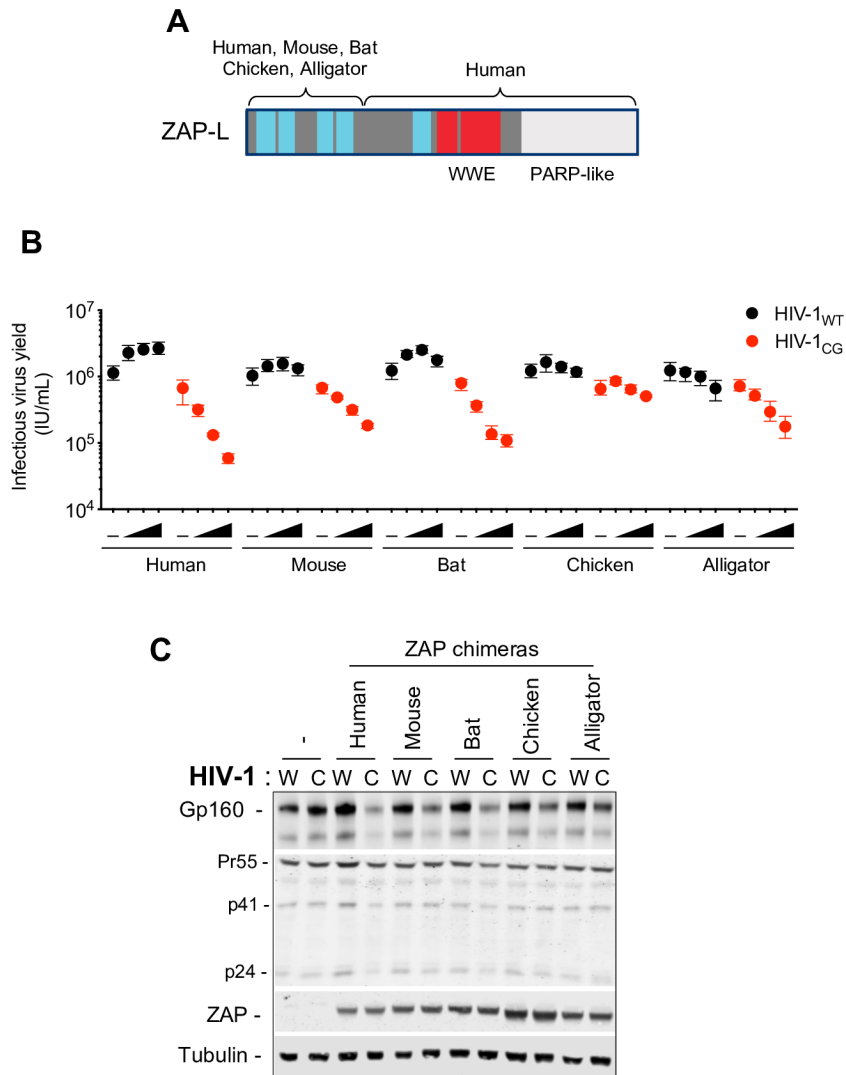
571 **Fig 2. Human PARP12 does not restrict CpG-rich viruses.** (A-B) HEK293T ZAP^{-/-} cells were
572 transfected with HIV-1_{WT} or HIV-1_{CG} plasmids and increasing amounts (0ng, 75ng, 145ng, or
573 290ng) of a plasmid encoding human ZAP-L-HA or PARP12-HA. Supernatant was harvested
574 after 48h and the infectious virus yield was determined using MT4-R5-GFP target cells (A).
575 Whole cell lysates were analysed by western blotting (B). IU, infectious units. (C) HEK293T
576 ZAP^{-/-} cells were transfected with plasmids encoding a luciferase reporter gene that contained
577 VSV-G wildtype (WT) or CG-enriched (VSV-G CG) sequences, or IAV-NP WT or CG-enriched
578 sequences as 3' UTRs, together with plasmids expressing ZAP-L, PARP12 or an empty
579 plasmid (vector). RLU, relative light units. (D) HEK293T ZAP^{-/-} cells were transfected with
580 plasmids expressing ZAP-L-3xHA or PARP12-3xHA and 24h later culture medium was
581 supplemented with 100μM 4SU. After overnight incubation cells were irradiated with UV light,
582 and ZAP-L/PARP12 were immunoprecipitated. RNA bound to each protein was radiolabeled
583 and protein-RNA adducts were resolved by SDS-PAGE, transferred to a nitrocellulose
584 membrane and exposed to autoradiographic film. In parallel, a western blot of
585 immunoprecipitated proteins was done using anti-HA antibody. IP, immunoprecipitation. IB,
586 immunoblot.

587



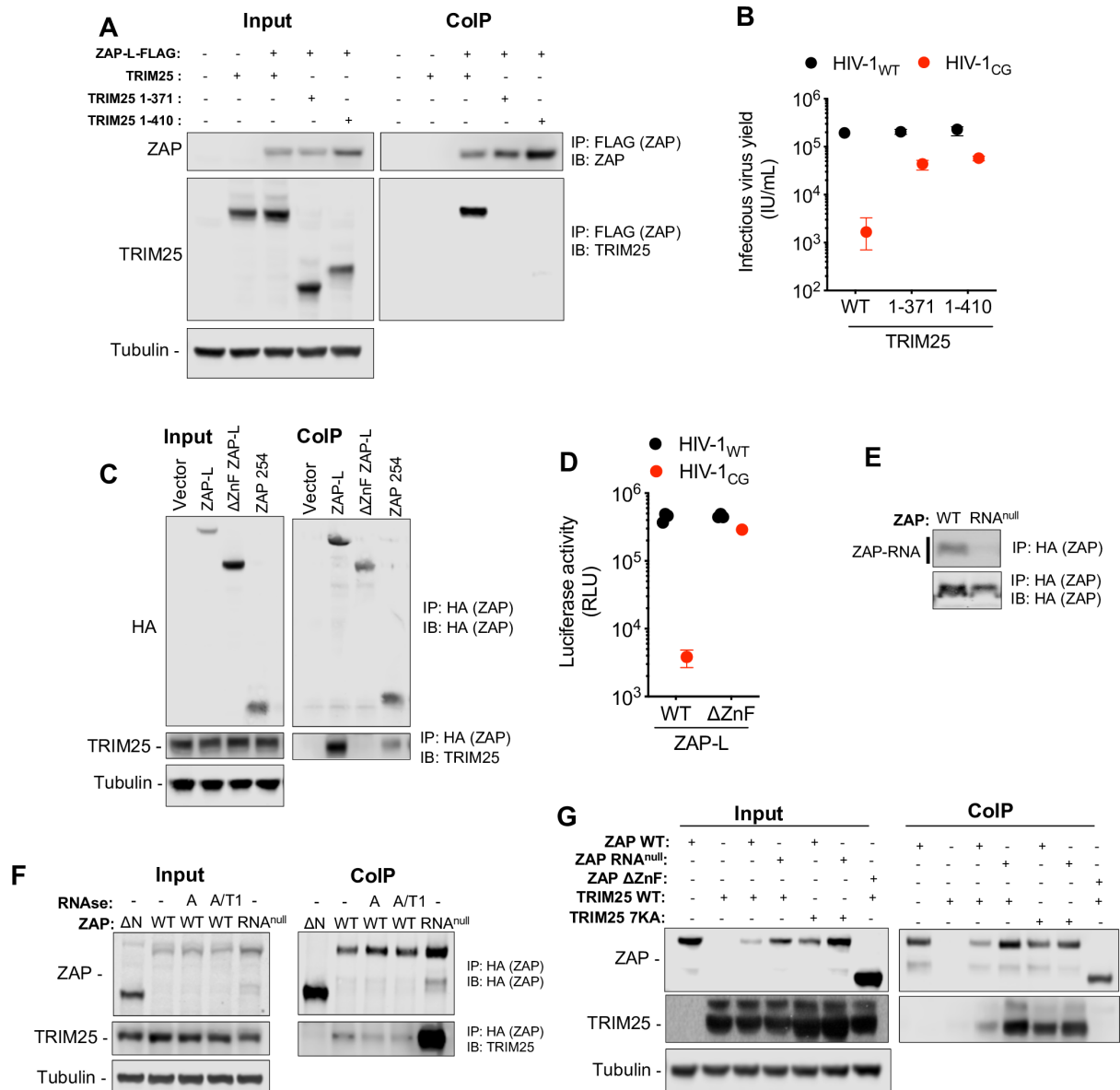
588
589
590
591
592
593
594
595
596
597

Fig 3. RNA transcripts from vertebrates are CpG-suppressed. (A) Open reading frames (ORFs) from several organisms belonging to the indicated phyla were collected from the NCBI nucleotide database and dinucleotide frequency ratio (observed/expected) was calculated and frequency distribution for each dinucleotide in ORFs was plotted. (B) Average dinucleotide observed/expected ratio in various animal species. Evolutionary distance (presented in million years, Ma) of indicated species was based on (34). (C) Average dinucleotide observed/expected ratio in various portions of vertebrate mRNA transcripts vertebrates.



598
599

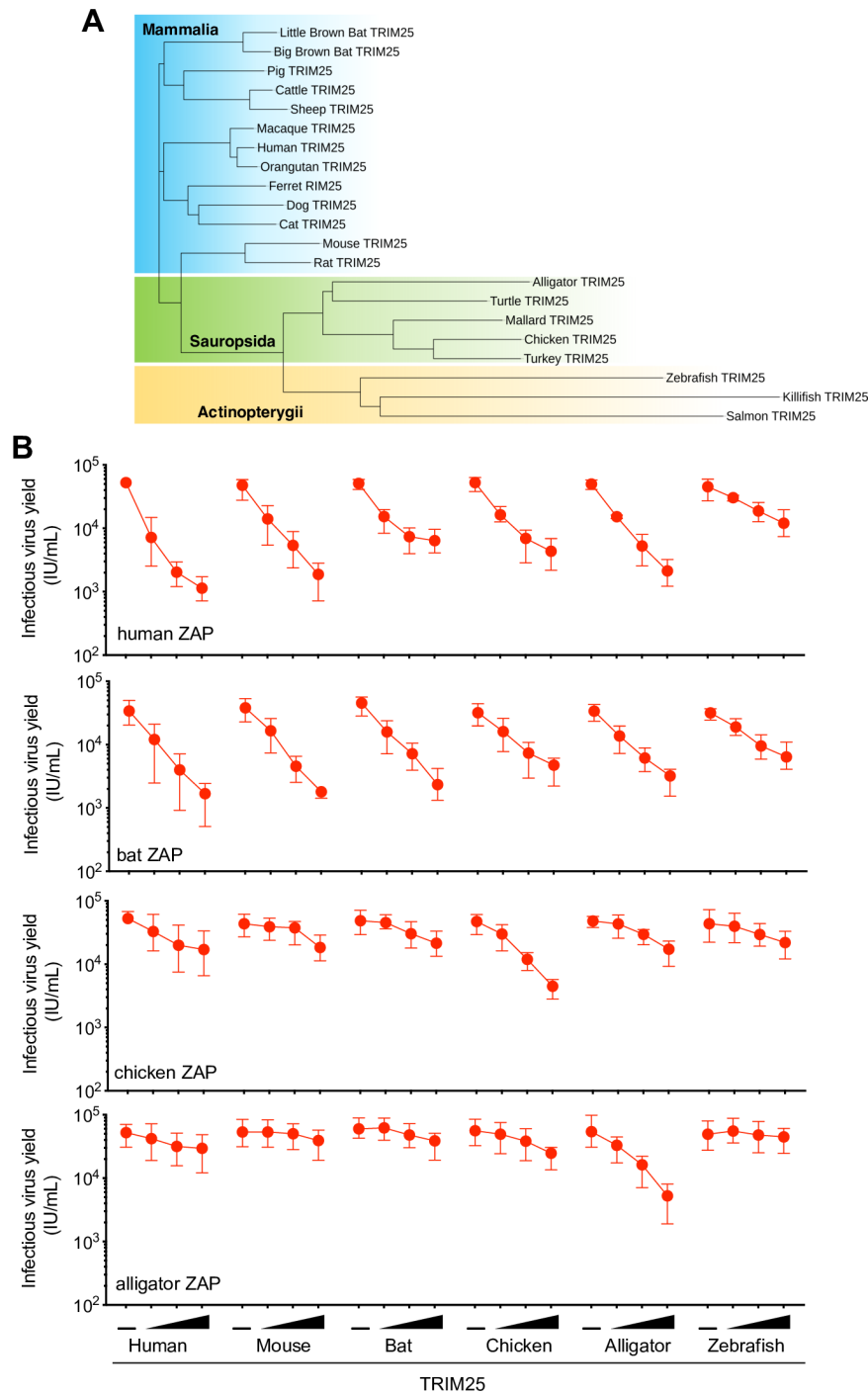
600 **Fig 4. ZAP protein antiviral activity in human cells.** (A) Schematic representation of ZAP
601 chimeras in which the RNA binding domain of mouse, bat, chicken and alligator ZAP was
602 fused to the WWE and PARP-like domain of human ZAP. (B-C) HEK293T ZAP^{-/-} cells were
603 transfected with HIV-1_{WT} (W) or HIV-1_{CG} (C) proviral plasmids and increasing amounts (0ng,
604 75ng, 145ng, or 290ng) of a plasmid encoding each ZAP chimera. Supernatant was harvested
605 after 48h and the infectious virus yield was determined using MT4-R5-GFP target cells (B).
606 Whole cell lysates were analysed by western blotting probing with antibodies against HIV-1
607 proteins and ZAP (C). -, Indicates co-transfection with an empty vector in place of a ZAP
608 expression plasmid.
609



610
611
612
613
614
615
616
617
618
619
620
621
622
623
624
625
626
627
628

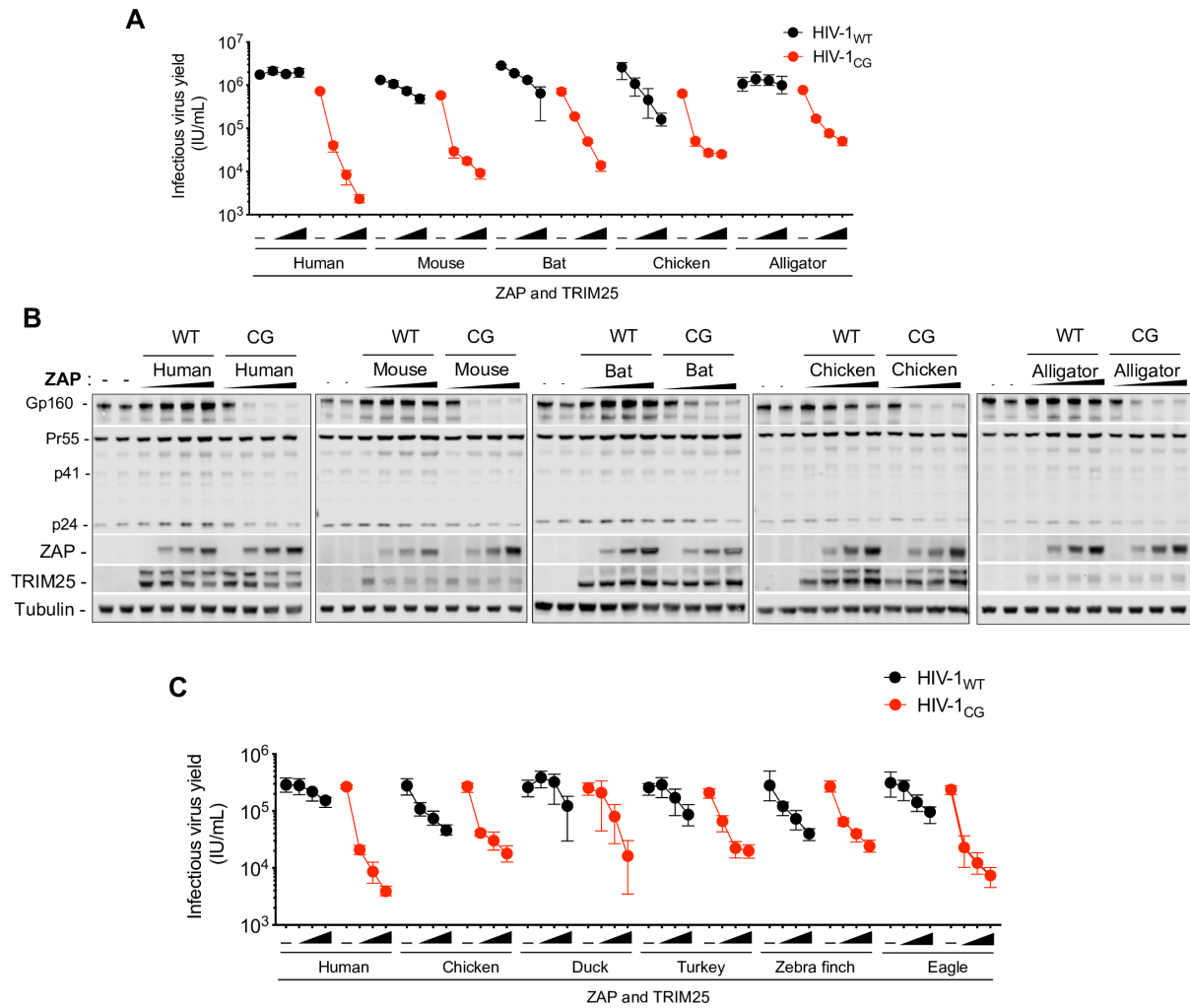
Fig 5. TRIM25 binds the ZAP NTD independently of RNA. (A) HEK293T ZAP^{-/-} and TRIM25^{-/-} cells were co-transfected with plasmids expressing human ZAP-L-FLAG and full-length untagged human TRIM25 or one of two human TRIM25 truncations (corresponding to the N-terminal 371 or 410 amino acids of TRIM25), that lack the SPRY domain (20). Proteins were immunoprecipitated from cell lysates with an anti-FLAG antibody and subjected to western blot analysis. IP, immunoprecipitation. IB, immunoblot. (B) HEK293T ZAP^{-/-} and TRIM25^{-/-} cells were co-transfected with proviral plasmids and plasmids encoding human ZAP and full-length TRIM25 or the indicated truncated TRIM25 proteins. Infectious virus yield was determined using MT4-R5-GFP target cells. (C) HEK293T ZAP^{-/-} cells were transfected with an empty vector or plasmids encoding human ZAP-L-HA, a truncated ZAP lacking the RNA binding domain (ΔZnF ZAP-L) or a truncated ZAP comprising the N-terminal 254 amino acids (ZAP 254). Proteins were immunoprecipitated from cell lysates with an anti-HA antibody and analysed by western blotting to detect overexpressed ZAP-L-HA and endogenous TRIM25. (D) Antiviral activity of ΔZnF ZAP-L was assessed by co-transfecting HEK293T ZAP^{-/-} cells with indicated proviral plasmids and plasmids encoding full length (WT) or truncated (ΔZnF) human ZAP. Infectious virus yield was determined using MT4-R5-GFP target cells. (E) HEK293T ZAP^{-/-} cells were transfected with plasmids encoding human ZAP-L (WT) or an

629 RNA-binding mutant of ZAP (RNA^{null}, R74A, R75A, K76A). After overnight incubation cells
630 were irradiated with UV light, and ZAP proteins were immunoprecipitated. RNA bound to each
631 protein was radiolabelled and protein-RNA adducts were resolved by SDS-PAGE, transferred
632 to a nitrocellulose membrane and exposed to autoradiographic film. In parallel, a western blot
633 of immunoprecipitated proteins was done using anti-HA antibody. IP, immunoprecipitation. IB,
634 immunoblot. (F) HEK293T ZAP^{-/-} cells were transfected with plasmids encoding HA-tagged
635 human ZAP-L (WT), Δ ZnF ZAP-L or ZAP (RNA^{null}). Cell lysates were treated with RNase A or
636 a mixture of RNase A and T1. ZAP protein complexes immunoprecipitated and subjected to
637 western blot analysis to detect overexpressed ZAP-L-HA and endogenous TRIM25. (G)
638 HEK293T ZAP^{-/-} and TRIM25^{-/-} cells were transfected with plasmids encoding HA-tagged
639 ZAP-L (WT), Δ ZnF ZAP-L or ZAP (RNA^{null}), along with untagged TRIM25 or a TRIM25 RNA
640 binding mutant (TRIM25 7KA). ZAP-HA protein complexes immunoprecipitated and subjected
641 to western blot analysis to detect overexpressed ZAP and TRIM25 proteins.



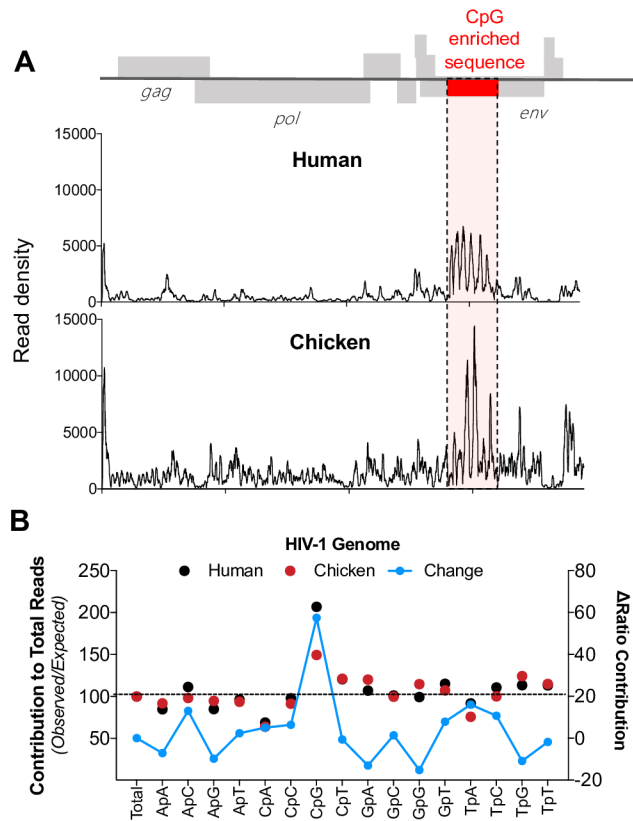
642
643
644
645
646
647
648
649
650
651
652

Fig 6. ZAP proteins from tetrapods have antiviral activity in the presence of cognate TRIM25. (A) Phylogenetic analysis of TRIM25 protein sequences from vertebrate species. Shaded areas indicate cluster sequences from mammals (in blue), birds and reptiles (in green) and ray-finned fish (in yellow). (B) HEK293T ZAP^{-/-} and TRIM25^{-/-} cells were co-transfected with an HIV-1_{CG} proviral plasmid as well as a fixed amount of a plasmid encoding human ZAP or ZAP chimeras. For each ZAP protein, cells were also co-transfected increasing amounts of a plasmid (0ng 10ng, 30ng or 90ng) expressing a TRIM25 protein from the 6 different indicated species. After 48h, infectious virus yield was determined using MT4-R5-GFP target cells.



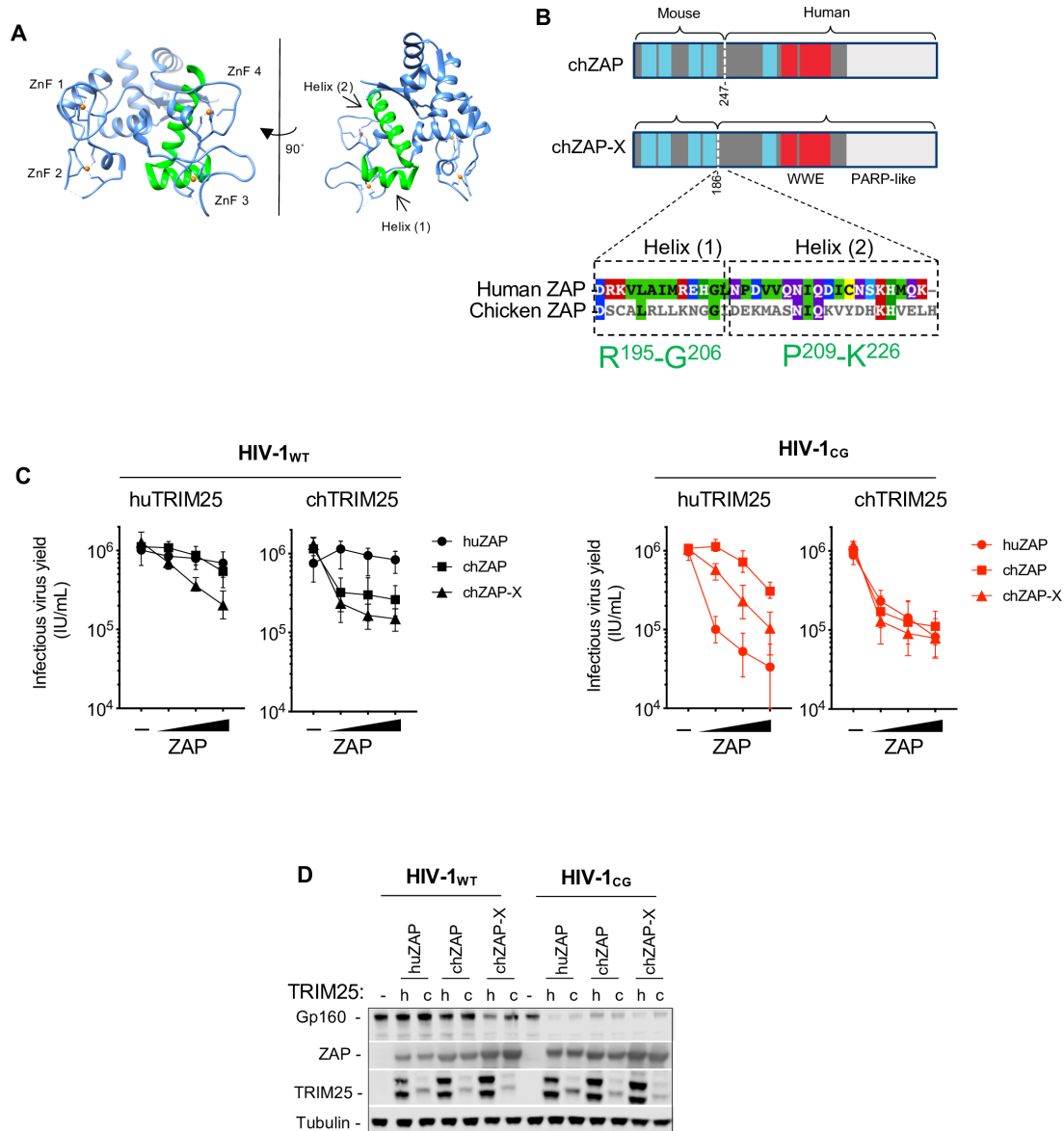
653
654

655 **Fig 7. Avian ZAP proteins are less selective for CpG enriched HIV-1.** (A-B) HEK293T
656 ZAP^{-/-} and TRIM25^{-/-} cells were co-transfected with indicated proviral plasmids, increasing
657 amounts (0ng, 75ng, 145ng, or 290ng) of a plasmid encoding an FLAG-tagged human ZAP
658 or mouse, bat, chicken and alligator ZAP chimeras and a fixed amount of a plasmid encoding
659 a cognate HA-TRIM25 protein. After 48h, infectious virus yield was determined using MT4-
660 R5-GFP target cells (A). Whole cell lysates were analysed by western blotting probing with
661 antibodies against HIV-1 proteins ZAP-FLAG and TRIM25-HA (B). (C) HE293T ZAP^{-/-} and
662 TRIM25^{-/-} cells were transfected with HIV-1 proviral plasmids, along with increasing amounts
663 (0ng, 75ng, 145ng, or 290ng) of a plasmids expressing human ZAP or ZAP chimeras from
664 various avian species. For cells transfected with human ZAP, a fixed amount of a human
665 TRIM25 expression plasmid was co-transfected, while for the avian ZAP chimeras, chicken
666 TRIM25 was used. After 48h, infectious virus yield was determined using MT4-R5-GFP target
667 cells.
668



669
670
671
672
673
674
675
676
677
678
679
680
681

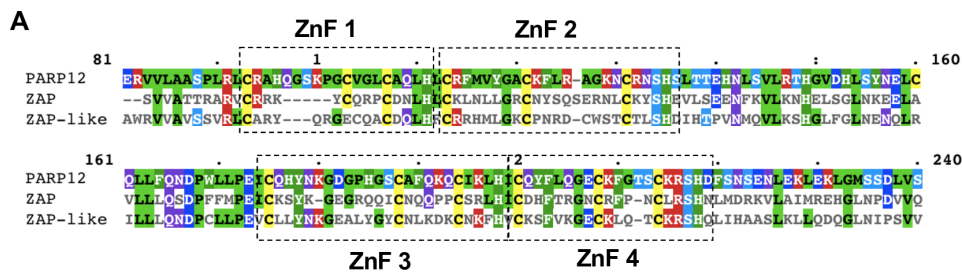
Fig 8. Differences in the RNA binding profiles of human and chicken ZAP. (A) HEK293T ZAP^{-/-} and TRIM25^{-/-} cells were transfected with an HIV-1_{CG} proviral plasmid and a plasmid expressing human ZAP or chicken ZAP chimera. Cells were treated with 4-thiouridine prior to UV-crosslinking and CLIP analysis. Reads associated with human (top) or chicken (bottom) ZAP were mapped to the HIV-1_{CG} genome and the read density plotted against position in the HIV-1_{CG} genome. CpG-enriched region the HIV-1_{CG} genome is highlighted in red and dashed lines. (B) Contribution (% observed/expected) for each dinucleotide to reads derived from the HIV-1_{CG} genome to was calculated. Shift in the ratio for each dinucleotide contribution comparing human and chicken ZAP reads was also determined (blue line).



682
683
684
685
686
687
688
689
690
691
692
693
694
695
696
697
698
699
700

Fig 9. A determinant in the ZAP NTD contributes to the species-specific cognate TRIM25 requirement. (A) Representation of the crystal structure of the RNA-binding NTD domain of human ZAP (PDB 6UEI, (11)). ZnF 1-4 indicate zinc fingers 1 through 4. Areas colored in green indicate α -helices 1 and 2 at the C-terminus of the NTD. (B, top) Schematic diagram of chicken ZAP (chZAP) chimera, containing the N-terminal 247 amino acids of chicken ZAP, in an otherwise human ZAP background, and chicken ZAP-X (chZAP-X) chimera, that contains the N-terminal 186 amino acids of chicken ZAP in a human ZAP background. chZAP-X contains the two human α -helices highlighted (A). (B, bottom) Sequence alignment of the α -helices 1 and 2 in human ZAP with the corresponding region in chicken ZAP. Colors indicate amino acid identity and conservation. The position numbers for the two α -helices in humanZAP are indicated in green. (C-D) HEK293T ZAP^{-/-} and TRIM25^{-/-} cells were co-transfected with HIV-1_{WT} and HIV-1_{CG} proviral plasmids, as well as plasmids encoding human ZAP (huZAP), chicken ZAP chimera (chZAP) and the chicken ZAP-X (chZAP-X) chimera and either human TRIM25 or chicken TRIM25. After 48h, infectious virus yield was determined using MT4-R5-GFP target cells (C). Whole cell lysates were analysed by western blotting probing with antibodies against HIV-1 proteins ZAP-FLAG and TRIM25-HA (D)

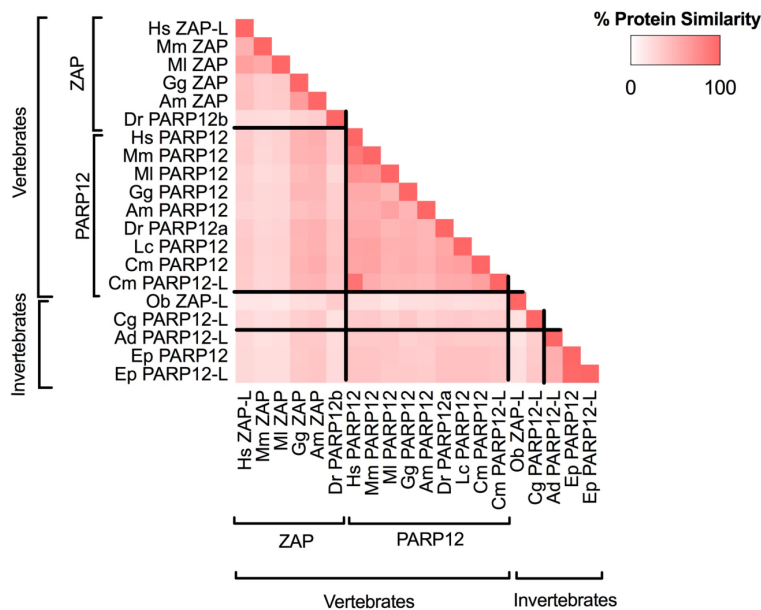
701
702



B Percentage Identity

	PARP12	ZAP	ZAP-like
PARP12	100		
ZAP	38.3	100	
ZAP-like	36.4	39.1	100

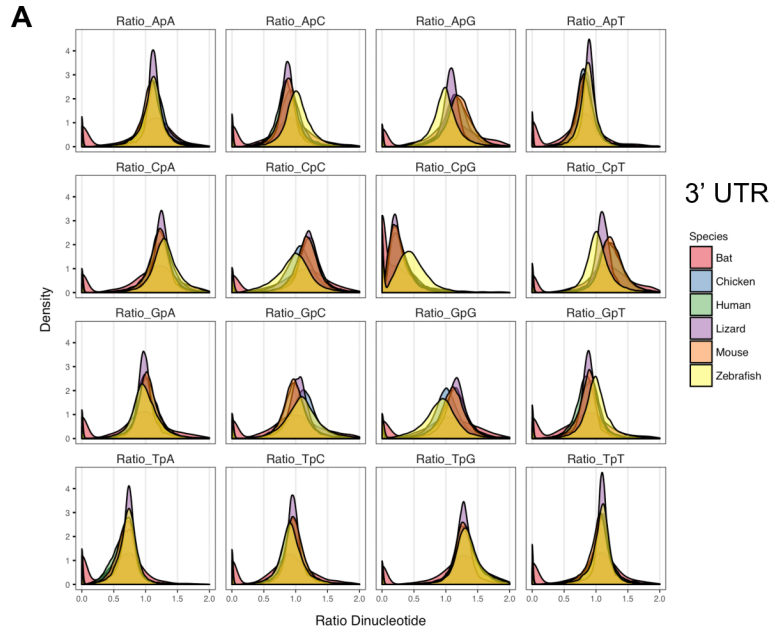
C



703
704

705 **S1 Fig. Homology among ZAP, PARP12 and ZAP-like proteins.** (A) Protein sequence
706 alignment of the N-terminal domain (NTDs) of human ZAP, PARP12 and ZAP-like protein.
707 Colored residues indicate amino acid properties and conservation. (B) Percentage identity
708 matrix among human ZAP, PARP12 and ZAP-like proteins. (C) Percentage protein similarity
709 one-to-one matrix among ZAP and PARP12 paralogues found in vertebrate and invertebrate
710 species. Hs, *Homo sapiens* (human); Mm, *Mus musculus* (mouse); Ml, *Myotis lucifugus* (little
711 brown bat), Gg, *Gallus gallus* (chicken); Am, *Alligator mississippiensis* (alligator); Dr, *Danio*
712 *rerio* (zebrafish); Lc, *Latimeria chalumnae* (Coelacanth); Ob, *Octopus bimaculoides* (California
713 two-spot octopus); Cg, *Crassostrea gigas* (oyster); Ad, *Acropora digitifera* (coral).

714



715

716

717

718

719

720

721

722

S2 Fig. Dinucleotide composition in mRNA 3'UTRs across vertebrates. (A) The 3' untranslated regions of mRNA transcripts found in transcriptomes of several vertebrates were collected from the NCBI nucleotide database and dinucleotide frequency ratio (observed/expected) was calculated and frequency distribution for each dinucleotide was plotted.

723 **REFERENCES**

- 724 1. Chow KT, Gale M, Loo Y-M. RIG-I and Other RNA Sensors in Antiviral Immunity.
725 *Annu Rev Immunol* [Internet]. 2018 Apr 20;36(1):667–94. Available from:
726 <https://doi.org/10.1146/annurev-immunol-042617-053309>
- 727 2. Schoggins JW. Interferon-Stimulated Genes: What Do They All Do? *Annu Rev Virol*
728 [Internet]. 2019 Sep 29;6(1):567–84. Available from: [https://doi.org/10.1146/annurev-](https://doi.org/10.1146/annurev-virology-092818-015756)
729 [virology-092818-015756](https://doi.org/10.1146/annurev-virology-092818-015756)
- 730 3. Gao G, Guo X, Goff SP. Inhibition of Retroviral RNA Production by ZAP, a CCCH-
731 Type Zinc Finger Protein. *Science (80-)* [Internet]. 2002 Sep 6;297(5587):1703 LP –
732 1706. Available from: <http://science.sciencemag.org/content/297/5587/1703.abstract>
- 733 4. Guo X, Carroll J-WN, MacDonald MR, Goff SP, Gao G. The Zinc Finger Antiviral
734 Protein Directly Binds to Specific Viral mRNAs through the CCCH Zinc Finger Motifs.
735 *J Virol* [Internet]. 2004 Dec 1;78(23):12781 LP – 12787. Available from:
736 <http://jvi.asm.org/content/78/23/12781.abstract>
- 737 5. Müller S, Möller P, Bick MJ, Wurr S, Becker S, Günther S, et al. Inhibition of Filovirus
738 Replication by the Zinc Finger Antiviral Protein. *J Virol* [Internet]. 2007 Mar
739 1;81(5):2391 LP – 2400. Available from: <http://jvi.asm.org/content/81/5/2391.abstract>
- 740 6. Li MMH, Lau Z, Cheung P, Aguilar EG, Schneider WM, Bozzacco L, et al. TRIM25
741 Enhances the Antiviral Action of Zinc-Finger Antiviral Protein (ZAP). *PLOS Pathog*
742 [Internet]. 2017 Jan 6;13(1):e1006145. Available from:
743 <https://doi.org/10.1371/journal.ppat.1006145>
- 744 7. Zheng X, Wang X, Tu F, Wang Q, Fan Z, Gao G. TRIM25 Is Required for the Antiviral
745 Activity of Zinc Finger Antiviral Protein. Diamond MS, editor. *J Virol* [Internet]. 2017
746 May 1;91(9):e00088-17. Available from: [http://jvi.asm.org/content/91/9/e00088-](http://jvi.asm.org/content/91/9/e00088-17.abstract)
747 [17.abstract](http://jvi.asm.org/content/91/9/e00088-17.abstract)
- 748 8. Guo X, Ma J, Sun J, Gao G. The zinc-finger antiviral protein recruits the RNA
749 processing exosome to degrade the target mRNA. *Proc Natl Acad Sci* [Internet]. 2007

- 750 Jan 2;104(1):151 LP – 156. Available from:
751 <http://www.pnas.org/content/104/1/151.abstract>
- 752 9. Ficarelli M, Wilson H, Pedro Galão R, Mazzon M, Antzin-Anduetza I, Marsh M, et al.
753 KHNYN is essential for the zinc finger antiviral protein (ZAP) to restrict HIV-1
754 containing clustered CpG dinucleotides. *Elife* [Internet]. 2019 Jul 9;8. Available from:
755 <https://elifesciences.org/articles/46767>
- 756 10. Takata MA, Gonçalves-Carneiro D, Zang TM, Soll SJ, York A, Blanco-Melo D, et al.
757 CG dinucleotide suppression enables antiviral defence targeting non-self RNA.
758 *Nature*. 2017;550(7674).
- 759 11. Meagher JL, Takata M, Gonçalves-Carneiro D, Keane SC, Rebendenne A, Ong H, et
760 al. Structure of the zinc-finger antiviral protein in complex with RNA reveals a
761 mechanism for selective targeting of CG-rich viral sequences. *Proc Natl Acad Sci*
762 [Internet]. 2019 Nov 26;116(48):24303 LP – 24309. Available from:
763 <http://www.pnas.org/content/116/48/24303.abstract>
- 764 12. Luo X, Wang X, Gao Y, Zhu J, Liu S, Gao G, et al. Molecular Mechanism of RNA
765 Recognition by Zinc-Finger Antiviral Protein. *Cell Rep* [Internet]. 2020 Jan 7;30(1):46-
766 52.e4. Available from: <https://doi.org/10.1016/j.celrep.2019.11.116>
- 767 13. Cooper DN, Gerber-Huber S. DNA methylation and CpG suppression. *Cell Differ*
768 [Internet]. 1985;17(3):199–205. Available from:
769 <http://www.sciencedirect.com/science/article/pii/0045603985904889>
- 770 14. Law JA, Jacobsen SE. Establishing, maintaining and modifying DNA methylation
771 patterns in plants and animals. *Nat Rev Genet* [Internet]. 2010 Mar;11(3):204–20.
772 Available from: <https://pubmed.ncbi.nlm.nih.gov/20142834>
- 773 15. Welsby I, Hutin D, Gueydan C, Kruys V, Rongvaux A, Leo O. PARP12, an interferon-
774 stimulated gene involved in the control of protein translation and inflammation. *J Biol*
775 *Chem* [Internet]. 2014/08/01. 2014 Sep 19;289(38):26642–57. Available from:
776 <https://pubmed.ncbi.nlm.nih.gov/25086041>

- 777 16. Atasheva S, Frolova EI, Frolov I. Interferon-Stimulated Poly(ADP-Ribose)
778 Polymerases Are Potent Inhibitors of Cellular Translation and Virus Replication. *J*
779 *Virol* [Internet]. 2014 Feb 15;88(4):2116 LP – 2130. Available from:
780 <http://jvi.asm.org/content/88/4/2116.abstract>
- 781 17. Atasheva S, Akhrymuk M, Frolova EI, Frolov I. New PARP gene with an anti-
782 alphavirus function. *J Virol* [Internet]. 2012/05/23. 2012 Aug;86(15):8147–60.
783 Available from: <https://pubmed.ncbi.nlm.nih.gov/22623789>
- 784 18. Li L, Zhao H, Liu P, Li C, Quanquin N, Ji X, et al. PARP12 suppresses Zika virus
785 infection through PARP-dependent degradation of NS1 and NS3 viral proteins. *Sci*
786 *Signal* [Internet]. 2018 Jun 19;11(535):eaas9332. Available from:
787 <https://pubmed.ncbi.nlm.nih.gov/29921658>
- 788 19. Pan D, Zhang L. Tandemly Arrayed Genes in Vertebrate Genomes. Bennetzen J,
789 editor. *Comp Funct Genomics* [Internet]. 2008;2008:545269. Available from:
790 <https://doi.org/10.1155/2008/545269>
- 791 20. Sanchez JG, Sparrer KMJ, Chiang C, Reis RA, Chiang JJ, Zurenski MA, et al.
792 TRIM25 Binds RNA to Modulate Cellular Anti-viral Defense. *J Mol Biol* [Internet].
793 2018;430(24):5280–93. Available from:
794 <http://www.sciencedirect.com/science/article/pii/S0022283618308477>
- 795 21. Choudhury NR, Heikel G, Trubitsyna M, Kubik P, Nowak JS, Webb S, et al. RNA-
796 binding activity of TRIM25 is mediated by its PRY/SPRY domain and is required for
797 ubiquitination. *BMC Biol* [Internet]. 2017;15(1):105. Available from:
798 <https://doi.org/10.1186/s12915-017-0444-9>
- 799 22. Jetz W, Thomas GH, Joy JB, Hartmann K, Mooers AO. The global diversity of birds in
800 space and time. *Nature* [Internet]. 2012;491(7424):444–8. Available from:
801 <https://doi.org/10.1038/nature11631>
- 802 23. Nielsen R, Bustamante C, Clark AG, Glanowski S, Sackton TB, Hubisz MJ, et al. A
803 Scan for Positively Selected Genes in the Genomes of Humans and Chimpanzees.

- 804 PLOS Biol [Internet]. 2005 May 3;3(6):e170. Available from:
805 <https://doi.org/10.1371/journal.pbio.0030170>
- 806 24. Grunewald ME, Chen Y, Kuny C, Maejima T, Lease R, Ferraris D, et al. The
807 coronavirus macrodomain is required to prevent PARP-mediated inhibition of virus
808 replication and enhancement of IFN expression. PLOS Pathog [Internet]. 2019 May
809 16;15(5):e1007756. Available from: <https://doi.org/10.1371/journal.ppat.1007756>
- 810 25. Karlberg T, Klepsch M, Thorsell A-G, Andersson CD, Linusson A, Schüler H.
811 Structural Basis for Lack of ADP-ribosyltransferase Activity in Poly(ADP-ribose)
812 Polymerase-13/Zinc Finger Antiviral Protein. J Biol Chem [Internet]. 2015 Mar
813 20;290(12):7336–44. Available from: <http://www.jbc.org/content/290/12/7336.abstract>
- 814 26. Kleine H, Poreba E, Lesniewicz K, Hassa PO, Hottiger MO, Litchfield DW, et al.
815 Substrate-Assisted Catalysis by PARP10 Limits Its Activity to Mono-ADP-
816 Ribosylation. Mol Cell [Internet]. 2008;32(1):57–69. Available from:
817 <http://www.sciencedirect.com/science/article/pii/S1097276508005455>
- 818 27. Bird AP, Taggart MH. Variable patterns of total DNA and rDNA methylation in
819 animals. Nucleic Acids Res [Internet]. 1980 Apr 11;8(7):1485–97. Available from:
820 <https://doi.org/10.1093/nar/8.7.1485>
- 821 28. Simmonds P, Xia W, Baillie JK, Mckinnon K. Modelling mutational and selection
822 pressures on dinucleotides in eukaryotic phyla – selection against CpG and UpA in
823 cytoplasmically expressed RNA and in RNA viruses. 2013;1–16.
- 824 29. Greenbaum BD, Levine AJ, Bhanot G, Rabadan R. Patterns of Evolution and Host
825 Gene Mimicry in Influenza and Other RNA Viruses. PLOS Pathog [Internet]. 2008 Jun
826 6;4(6):e1000079. Available from: <https://doi.org/10.1371/journal.ppat.1000079>
- 827 30. Babayan SA, Orton RJ, Streicker DG. Predicting reservoir hosts and arthropod
828 vectors from evolutionary signatures in RNA virus genomes. Science (80-) [Internet].
829 2018 Nov 2;362(6414):577 LP – 580. Available from:
830 <http://science.sciencemag.org/content/362/6414/577.abstract>

- 831 31. Liberatore RA, Bieniasz PD. Tetherin is a key effector of the antiretroviral activity of
832 type I interferon in vitro and in vivo. *Proc Natl Acad Sci* [Internet]. 2011 Oct
833 19;201113694. Available from:
834 <http://www.pnas.org/content/early/2011/10/18/1113694108.abstract>
- 835 32. Busnadiego I, Kane M, Rihn SJ, Preugschas HF, Hughes J, Blanco-Melo D, et al.
836 Host and viral determinants of Mx2 antiretroviral activity. *J Virol* [Internet]. 2014/04/23.
837 2014 Jul;88(14):7738–52. Available from: <https://pubmed.ncbi.nlm.nih.gov/24760893>
- 838 33. Suchard MA, Lemey P, Baele G, Ayres DL, Drummond AJ, Rambaut A. Bayesian
839 phylogenetic and phylodynamic data integration using BEAST 1.10. *Virus Evol*
840 [Internet]. 2018 Jun 8;4(1). Available from: <https://doi.org/10.1093/ve/vey016>
- 841 34. Inoue JG, Miya M, Lam K, Tay B-H, Danks JA, Bell J, et al. Evolutionary Origin and
842 Phylogeny of the Modern Holocephalans (Chondrichthyes: Chimaeriformes): A
843 Mitogenomic Perspective. *Mol Biol Evol* [Internet]. 2010 Nov 1;27(11):2576–86.
844 Available from: <https://doi.org/10.1093/molbev/msq147>
- 845 35. Simmonds P. SSE: a nucleotide and amino acid sequence analysis platform. *BMC*
846 *Res Notes* [Internet]. 2012;5(1):50. Available from: [https://doi.org/10.1186/1756-0500-](https://doi.org/10.1186/1756-0500-5-50)
847 [5-50](https://doi.org/10.1186/1756-0500-5-50)
- 848 36. Kutluay SB, Zang T, Blanco-Melo D, Powell C, Jannain D, Errando M, et al. Global
849 Changes in the RNA Binding Specificity of HIV-1 Gag Regulate Virion Genesis. *Cell*
850 [Internet]. 2014;159(5):1096–109. Available from:
851 <http://www.sciencedirect.com/science/article/pii/S0092867414013014>

852

853